Supporting Information

A Curtin–Hammett Paradigm for Stereocontrol in Organocatalysis by Diarylprolinol Ether Catalysts

Jordi Burés,[a] Alan Armstrong,[b] Donna G. Blackmond[a]*

[a] Department of Chemistry, The Scripps Research Institute, La Jolla, CA 92037, US
[b] Department of Chemistry, Imperial College London SW72AZ, UK

blackmond@scripp.edu

Table of Contents:

1. Materials and general procedures

Dry toluene and $CHCl_3$ were obtained by passing the previously degassed solvents through activated alumina column. Toluene-d8 was purchased from Cambridge Isotope Laboratories, Inc. (D, 99.5%) in ampoules of 1 mL. $CDCl_3$ was purchased from Cambridge Isotope Laboratories, Inc. (D, 99.5%) in bottles of 100 g. Propanal (97%), 2-phenylpropanal (95%), isobutyraldehyde (98%) and isovaleraldehyde were purchased from Alfa Aesar and they were always carefully distilled prior to use. (*S*)-(–)-α,α-Diphenyl-2-pyrrolidinemethanol trimethylsilyl ether, (*S*)-α,α-bis[3,5-bis(trifluoromethyl)phenyl-2-pyrrolidinemethanol trimethylsilyl ether and *N*-phenylmaleimide were purchased from Sigma-Aldrich. (2*R*,5*R*)-2,5-Diphenylpyrrolidine was purchased from TCI America.

NMR spectra were recorded on Bruker DRX-600 equipped with a 5 mm DCH cryoprobe, DRX-500, and AMX-400 instruments and calibrated using residual undeuterated solvent as an internal reference.

The chiral GC were registered in an Agilent 7890A/ FID detector fitted with a VARIAN CP-ChiraSil-DEX CB 25 x 0.25. Column conditions: He, pressure = 15psi, initial temperature = 30 °C, final temperature = 60 °C, warming rate = 0.5 °C/min, detector temperature = 300 °C, injector temperature = 130 °C.

2. Enamine formation and Michael addition of isobutyraldehyde

100 µL (0.06 mmol) of a 0.6 M solution of (S)-(–)-α,α-diphenyl-2-pyrrolidinemethanol-trimethylsilyl ether in toluene-d8 were added to 0.5 mL (0.72 mmol) of a 1.44 M solution of isobutyraldehyde. The first spectra registered 200 seconds after the addition of the catalyst shows almost an equilibrated enamine/free catalyst ratio (0.43).

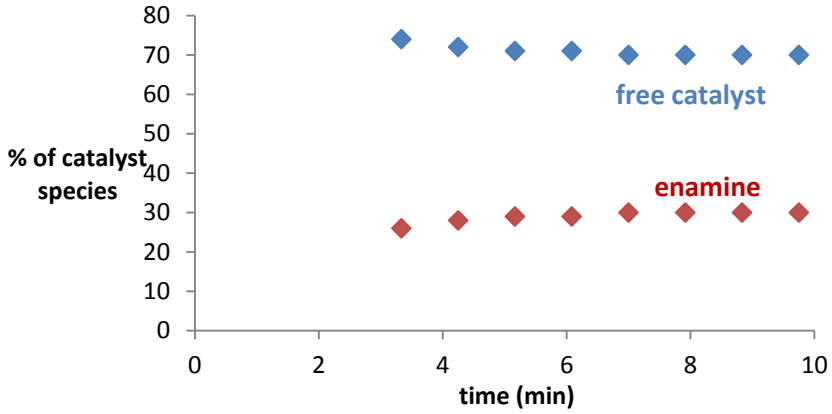

Figure 1. The equilibrium between free catalyst and enamine is achieved in less than 10 min.

The characteristic signals used to identify the enamine of the isobutyraldehyde were: –0.13 (9H, s), 1.64 (3H, d, *J*=1.4), 1.66 (3H, d, *J*=1.4), 5.79 (1H, hept, *J*=1.4).

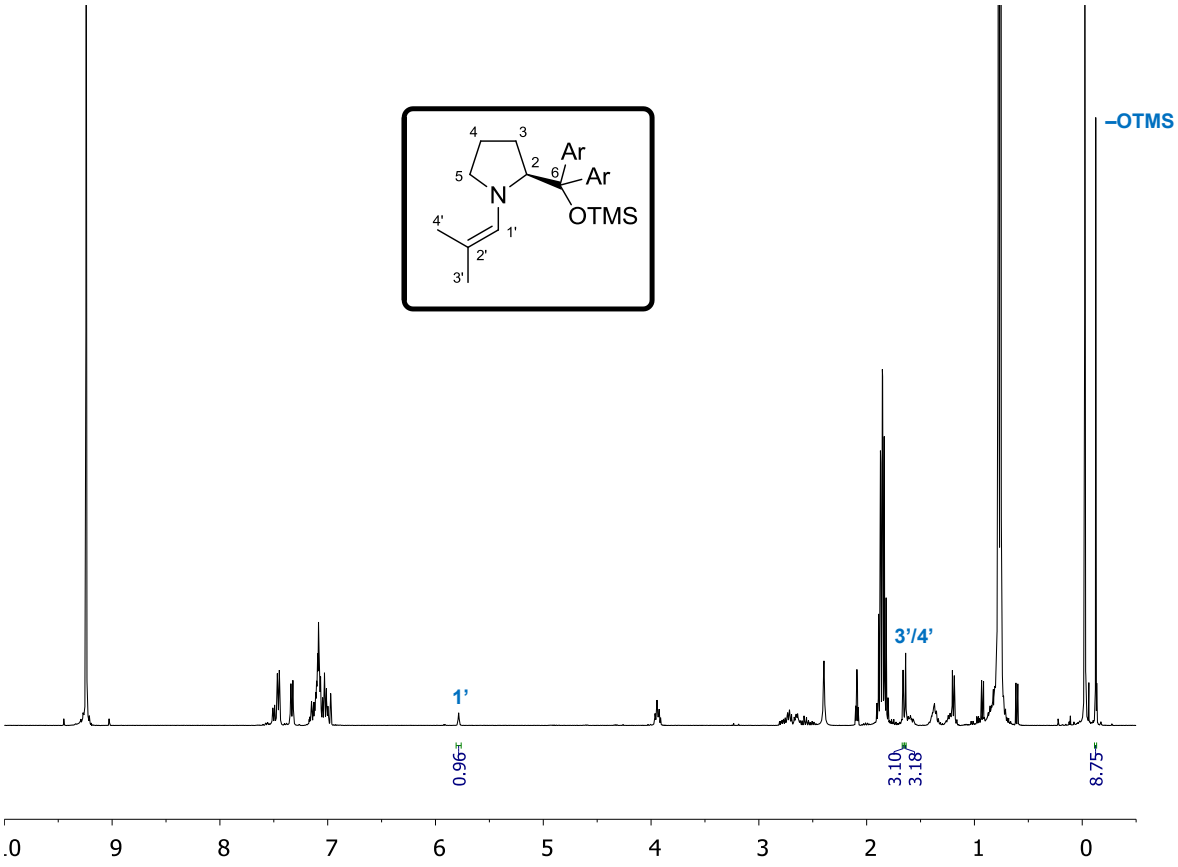

100 µL (0.06 mmol) of a 0.6 M solution of (*S*)-(–)-α,α-diphenyl-2-pyrrolidinemethanol-trimethylsilyl ether in toluene-d8 were added to 0.4 mL (0.60 mmol of *β*-nitrostyrene and 0.72

mmol of isobutyraldehyde) of a solution of β-nitrostyrene (1.5 M) and isobutyraldehyde (1.8 M) in toluene-d8. After 40 min the formation of the cyclobutane **5a** was quantitative, but no Michael product was observed. After 24 h the reaction was almost unaltered.

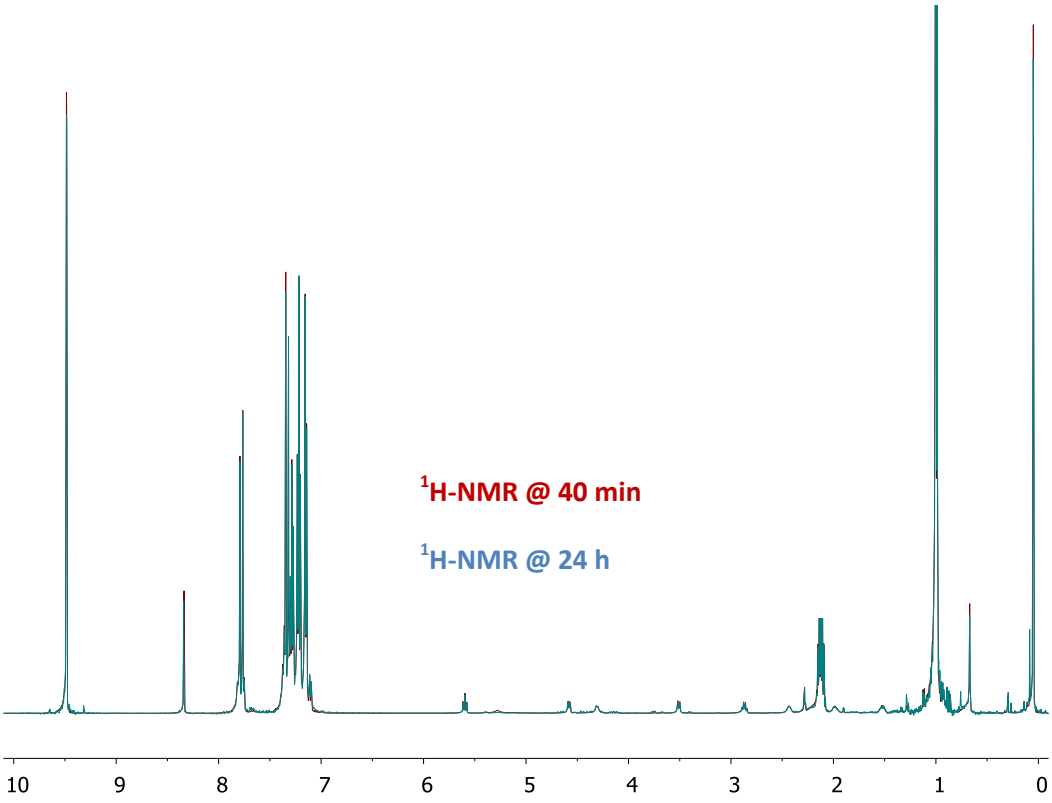

3. Kinetic isotopic effect in the Michael addition

The α,α-propanal-d2 was prepared following the experimental procedure described by Barefield.[1]

Measurements were performed using an Omnical Insight reaction calorimeter, which allows continuous monitoring of the instantaneous heat absorbed or released by a chemical reaction occurring in the vessel. The sample vessel is a 16 mL septum-cap vial equipped with a magnetic stirring bar. The system operates as a differential scanning calorimeter by comparing the heat released or consumed in a sample vessel with that from a reference compartment at intervals of 3 seconds over the course of the reaction.

The reactions were set up from common stock solutions:

Stock solution A: 1.0099 g of (*S*)-α,α-diphenyl-2-pyrrolidinemethanol trimethylsilyl, total volume of 2 mL of dry toluene.
Stock solution B: 2.2829 g of nitrostyrene, total volume of 5 mL of dry toluene.
Stock solution C: 1.0454 g of propanal, total volume of 5 mL of dry toluene.
Stock solution D: 1.0816 g of α,α-propanal-d2, total volume of 5 mL of dry toluene.
Stock solution E: 0.4504 g of acetic acid, total volume of 1 mL of dry toluene.
Stock solution F: 0.4806 g of acetic acid-d4, total volume of 1 mL of dry toluene.

Reaction propanal/CH_3COOH/H_2O: 500 µL of SL B + 500 µL of SL C + 380 µL of dry toluene + 13.5 µL of H_2O, then injection of 120 µL of a solution made from 200 µL of SL A + 40 µL of SL E.

Reaction propanal/CD_3COOD/D_2O: 500 µL of SL B + 500 µL of SL C + 380 µL of dry toluene + 13.5 µL of D_2O, then injection of 120 µL of a solution made from 200 µL of SL A + 40 µL of SL F.

Reaction α,α-propanal-d2/CD_3COOD/D_2O: 500 µL of SL B + 500 µL of SL D + 380 µL of dry toluene + 13.5 µL of D_2O, then injection of 120 µL of a solution made from 200 µL of SL A + 40 µL of SL F.

The results are summarized in the following figures.

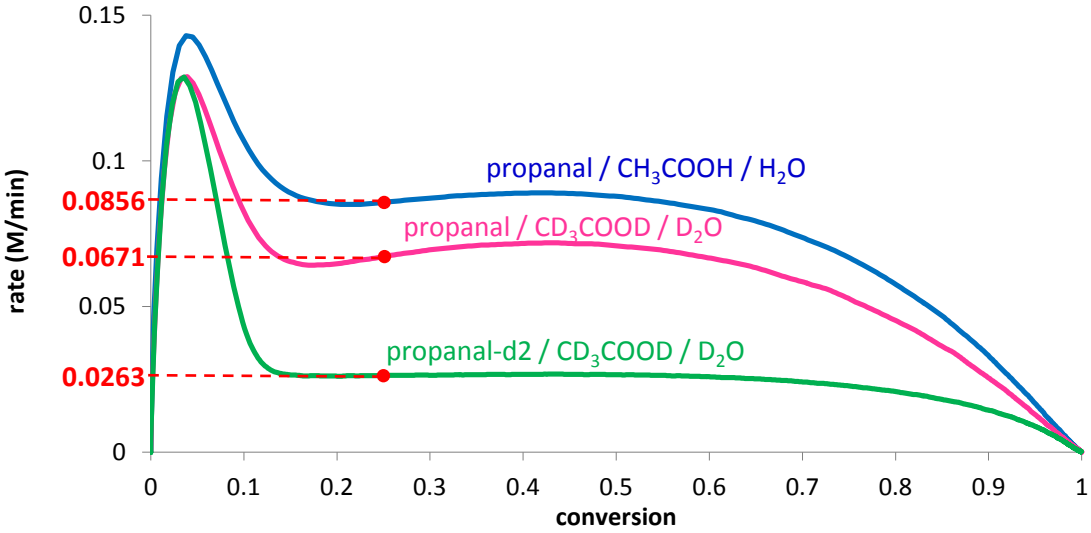

Figure 2. Rates measured by calorimetry for the different reactions.

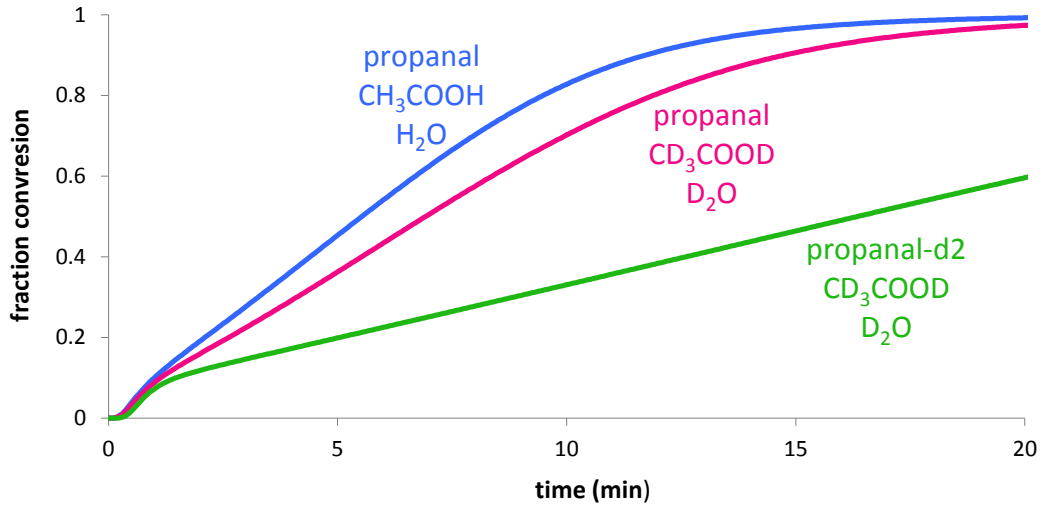

Figure 3. Processed calorimetry data to show the zero order kinetics.

4. Relationships of KIE for a reaction via a non-accumulating intermediate

In a two-stage reaction, via a non-accumulating intermediate the relationship of the rate constant (k_{obs}) obtained in steady state is:

$$\mathbf{A}^{\ominus} + \mathbf{5a} \underset{k_{-5a}}{\overset{k_{5a}}{\rightleftharpoons}} \mathbf{6} + \mathbf{AH} \xrightarrow{k_6} \mathbf{7}$$

$$\text{rate} = \frac{d[\mathbf{7}]}{dt} = k_6[\mathbf{6}][\mathbf{AH}]$$

Steady State Approximation:

$$0 = \frac{d[\mathbf{6}]}{dt} = k_{5a}[\mathbf{5a}][\mathbf{A}^-] - (k_{-5a} + k_6)[\mathbf{6}][\mathbf{AH}]$$

$$[\mathbf{6}] = \frac{k_{5a}}{k_{-5a}+k_6}\frac{[\mathbf{5a}][\mathbf{A}^-]}{[\mathbf{AH}]}$$

$$\text{So: rate} = \frac{k_{5a}k_6}{k_{-5a}+k_6}[\mathbf{5a}][\mathbf{A}^-] = k_{obs}[\mathbf{5a}][\mathbf{A}^-], \text{ where } \boldsymbol{k_{obs}} = \frac{\boldsymbol{k_{5a}k_6}}{\boldsymbol{k_{-5a}} + \boldsymbol{k_6}}$$

So, as is described in the reference 14 of the manuscript[7] via a non-accumulating intermediate in steady state either step, or both, may show isotopic sensitivity.

$$\frac{k_{obs}^{\mathrm{H}}}{k_{obs}^{\mathrm{D}}} = \frac{k_{5a}^{\mathrm{H}}}{k_{5a}^{\mathrm{D}}} \cdot \frac{k_6^{\mathrm{H}}}{k_6^{\mathrm{D}}} \cdot \frac{(k_{-5a}^{\mathrm{D}} + k_6^{\mathrm{D}})}{(k_{-5a}^{\mathrm{H}} + k_6^{\mathrm{H}})}$$

5. EXSY evidence of the equilibrium between 5a and 6

The cyclobutane prepared with an excess of catalyst and molecular sieves, as we described recently,[2] shows EXSY cross-peaks with a minor species, in equilibrium with the cyclobutane, that is present at lower concentration over the reaction. The complete assignment of this species is not possible because the signals are tiny and broad since it is unstable and it is exchanging really fast with the cyclobutane. Despite everything, it was possible to detect the same EXSY peaks when a NOESY experiment was registered during the reaction in standard conditions ([propanal]=1.2 M, [nitrostyrene]=1.0 M, [diphenylpropanolTMS]=0.1 M in toluene-d8).

The chemical shifts of the signals for the new species were determined and compared with the shifts of the signals for the cyclobutane thanks to these EXSY cross-peaks. It is important to point out that the two protons attached to the carbon atoms that change the hybridation from sp^3 to sp^2 were the most affected. In addition, some differences were observed in the rest of the hydrogen atoms surrounding these atoms, but not for the proton that has to be removed to generate the enamine. This is a strong suggestion that this atom is not present in the molecule in equilibrium with the cyclobutane.

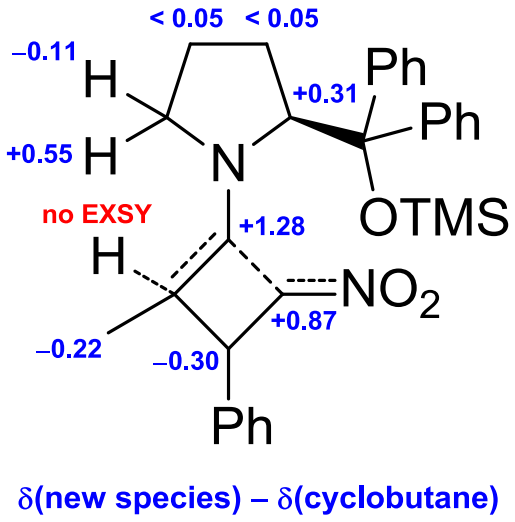

Figure 4. Difference in chemical shifts between the known cyclobutane and the new intermediate.

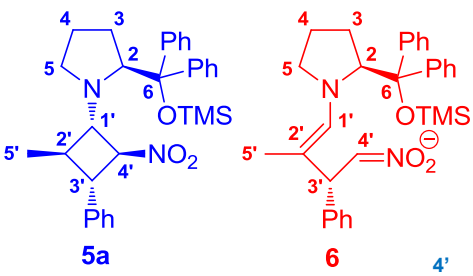

5a

6

Figure 5. NOESY of the cyclobutane (5a) prepared with an excess of catalyst (3) and MS.

Figure 6. NOESY recorded during a reaction in standard conditions.

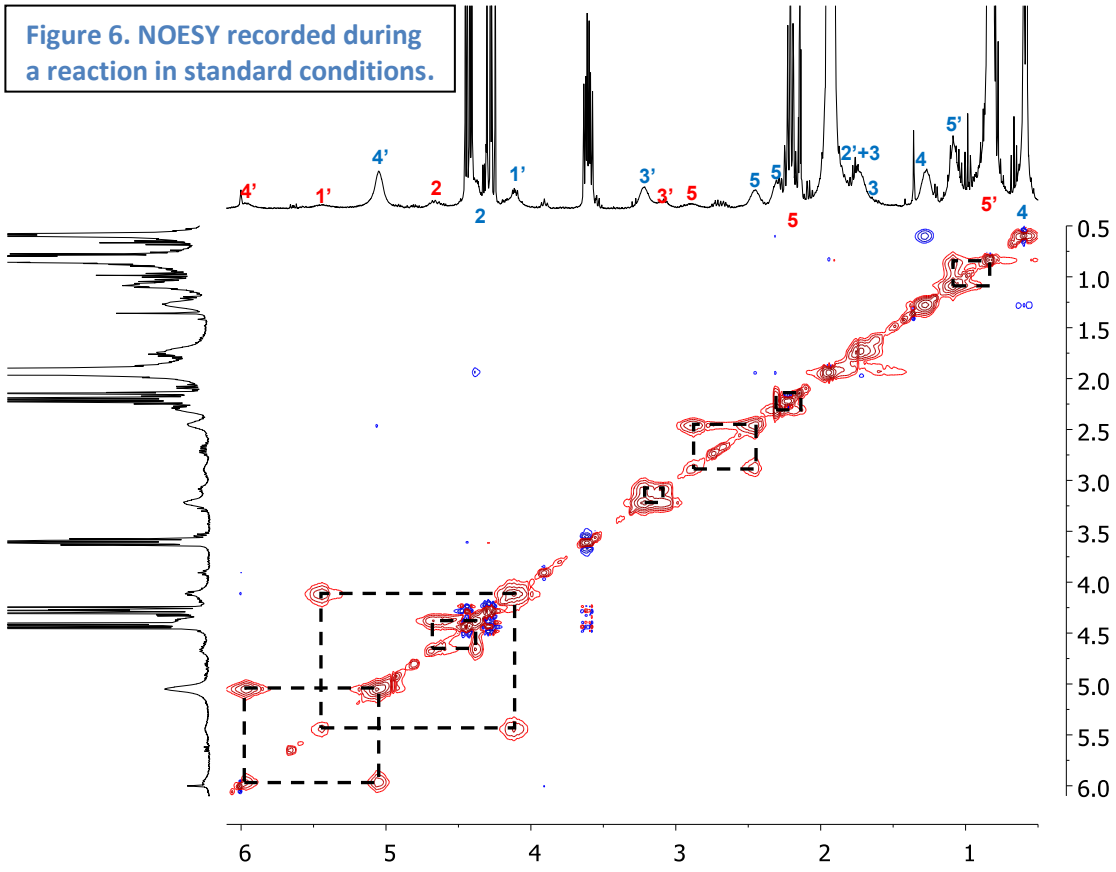

The EXSY cross-peaks were not present when isobutyraldehyde was used instead of propanal. This fact agrees with the previous assignment that the specie in equilibrium with the cyclobutane is the enamine nitronate, which in this case cannot be formed.

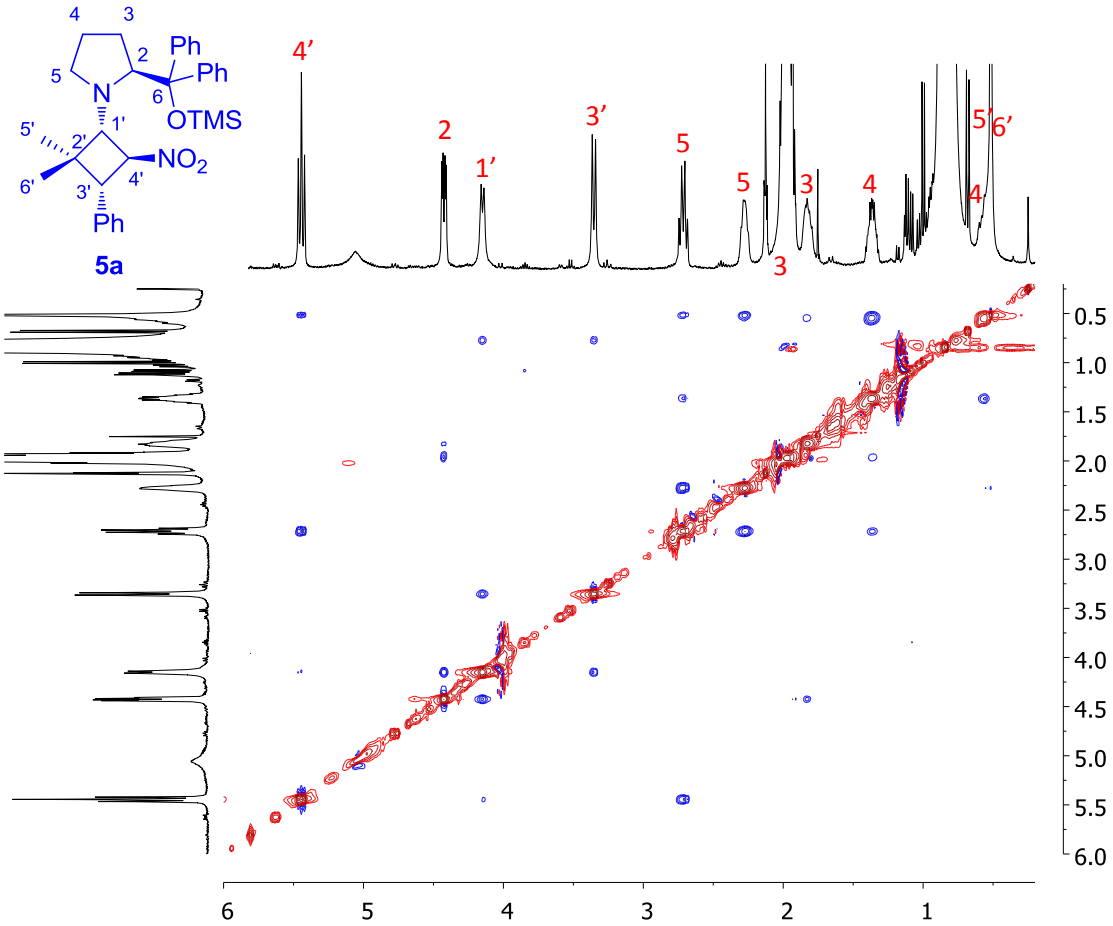

Figure 7. NOESY of cyclobutane (4b) and the catalyst (3) without EXSY peaks.

6. EXSY experiments of (2*R*,3*S*)-2-methyl-4-nitro-3-phenylbutanal

The thermodynamic ratio between the *syn* (2*R*,3*S*) and *anti* (2*S*,3*S*) diastereoisomers, product of the epimerization of the stereocenter in α to the aldehyde, is 60:40. In the presence of catalyst only the *E* enamine could be identified by NMR.

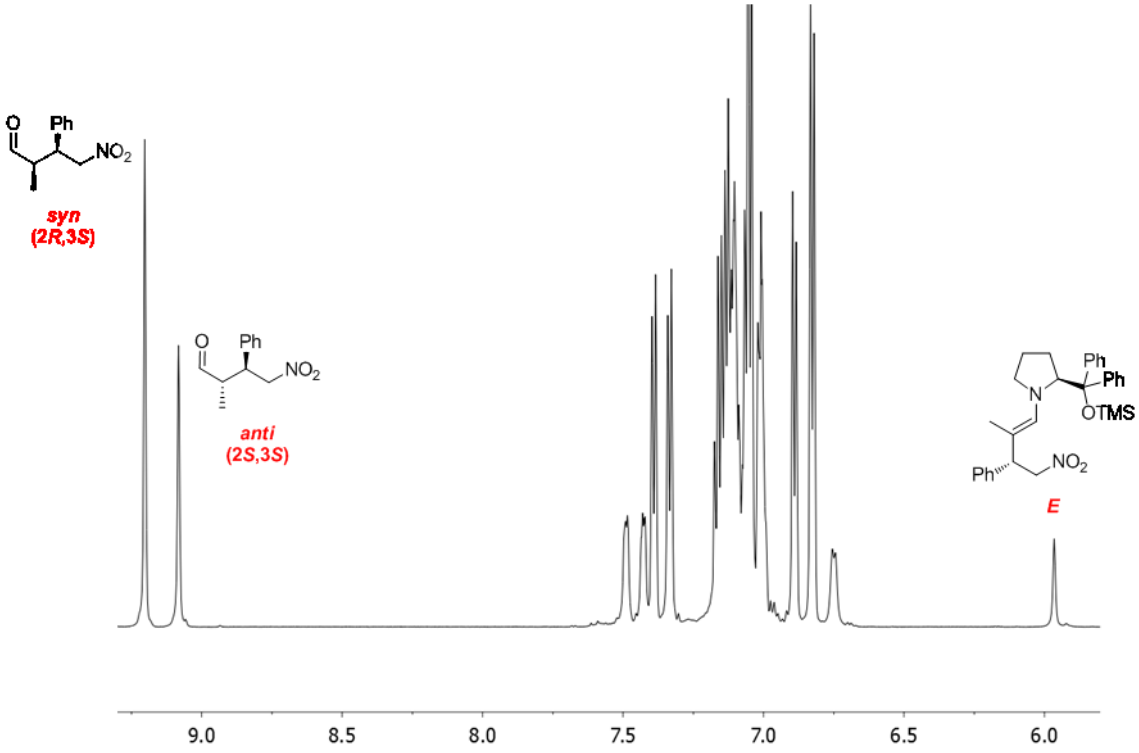

When acetic acid was added to the final mixture the *syn*/*anti* ratio was not affected, but the equilibrium was faster and it was possible to observe the interchange by EXSY. When the *E*-enamine peak was irradiated using a 1D-goesy sequence with different mixing times (τ_m), the peak corresponding to the *syn* diastereoisomer was much more intense than the *anti*.

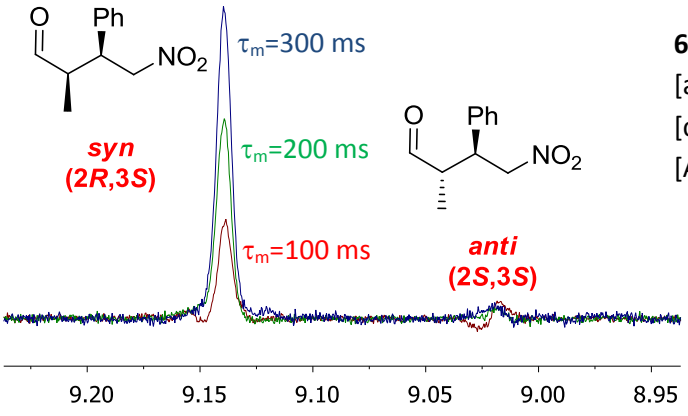

600 MHz
[aldehyde] = 0.87 M
[catalyst]=0.36 M
[AcOH]=0.66 M

This result shows that at least the protonation of the enamine is highly stereoselective and it is the main reason why the product does not epimerize very fast.

7. COPASI models

We used COPASI[3] to predict the epimerization rate for a selective process or for a non-selective process with this scheme of reaction:

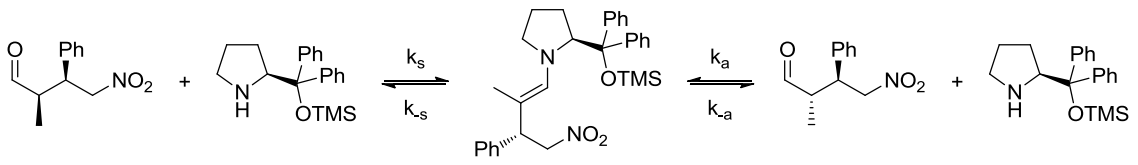

The value of k_s was estimated from the experimental NMR data of enamine appearance.

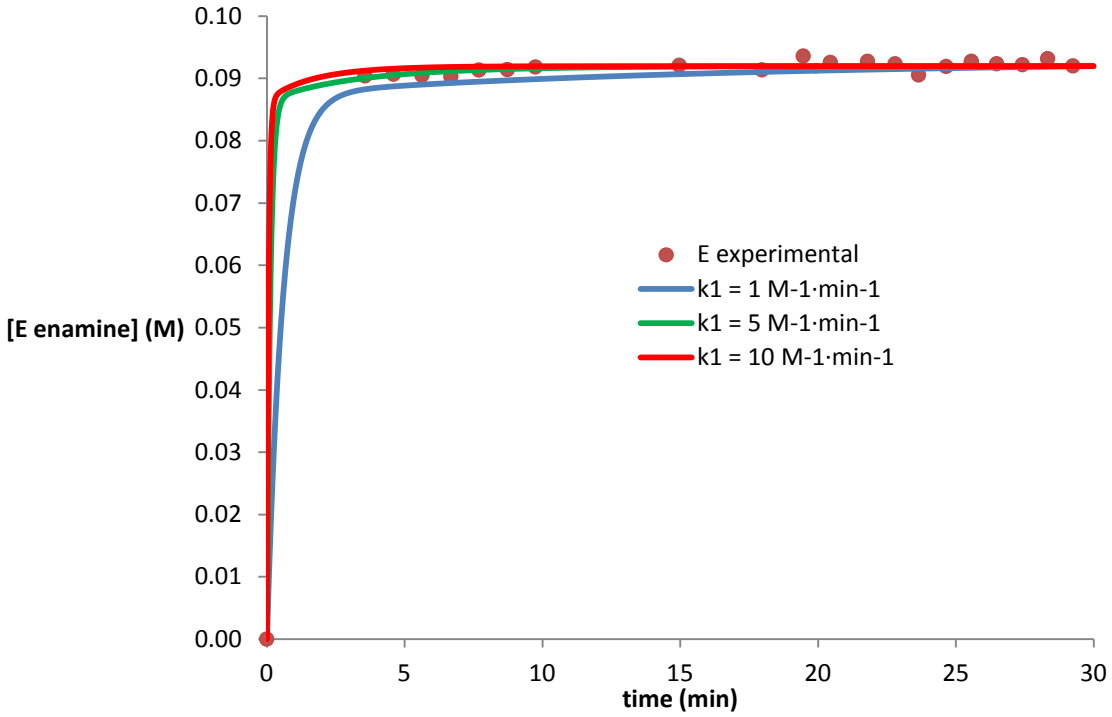

Because the formation of the enamine is too fast we cannot measure the exact value of k_s, but we can be sure that it is higher than 1.0 M^{-1} min^{-1}.

In our system, we measured by NMR the concentration of each species at initial time and the equilibrium.

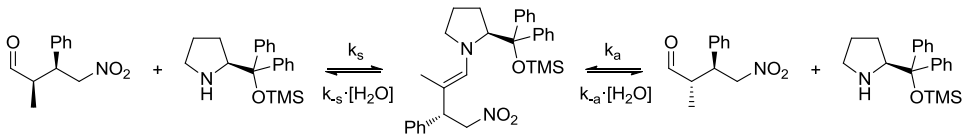

	syn-**4a**	**3**	*E*-**7**	*anti*-**4a**	**3**
initial	0.93 M	0.115 M	0.0 M	0.07 M	0.115 M
equilibrium	0.57 M	0.033 M	0.060 M	0.37 M	0.033 M

In the equilibrium:

$$0 = \frac{d[syn-\mathbf{4a}]}{dt} = k_{-s}[E-\mathbf{7}]_{eq} - k_s[syn-\mathbf{4a}]_{eq}[\mathbf{3}]_{eq}$$

$$\frac{k_s}{k_{-s}\cdot[\mathrm{H_2O}]} = \frac{[E-\mathbf{7}]_{eq}}{[syn-\mathbf{4a}]_{eq}[\mathbf{3}]_{eq}} = 3.19$$

$$0 = \frac{d[anti-\mathbf{4a}]}{dt} = k_{-a}[E-\mathbf{7}]_{eq} - k_a[anti-\mathbf{4a}]_{eq}[\mathbf{3}]_{eq}$$

$$\frac{k_a}{k_{-a}\cdot[\mathrm{H_2O}]} = \frac{[E-\mathbf{7}]_{eq}}{[anti-\mathbf{4a}]_{eq}[\mathbf{3}]_{eq}} = 4.91$$

7.1. Non-selective epimerization of (2*R*,3*S*)-2-methyl-4-nitro-3-phenylbutanal

In a non-selective process:

$$k_{-s} = k_{-a}$$

So, all the kinetic constants would be function of only one constant:

$$k_s = 1.00\ \mathrm{M^{-1}min^{-1}};\ k_{-s} = k_{-a} = \frac{k_s}{3.19} = 0.31\ \mathrm{M^{-1}min^{-1}}\ ;k_a = \frac{4.91}{3.19}k_s = 1.54\ \mathrm{M^{-1}min^{-1}}$$

And the result shows that the equilibrium is achieved in 100 min.

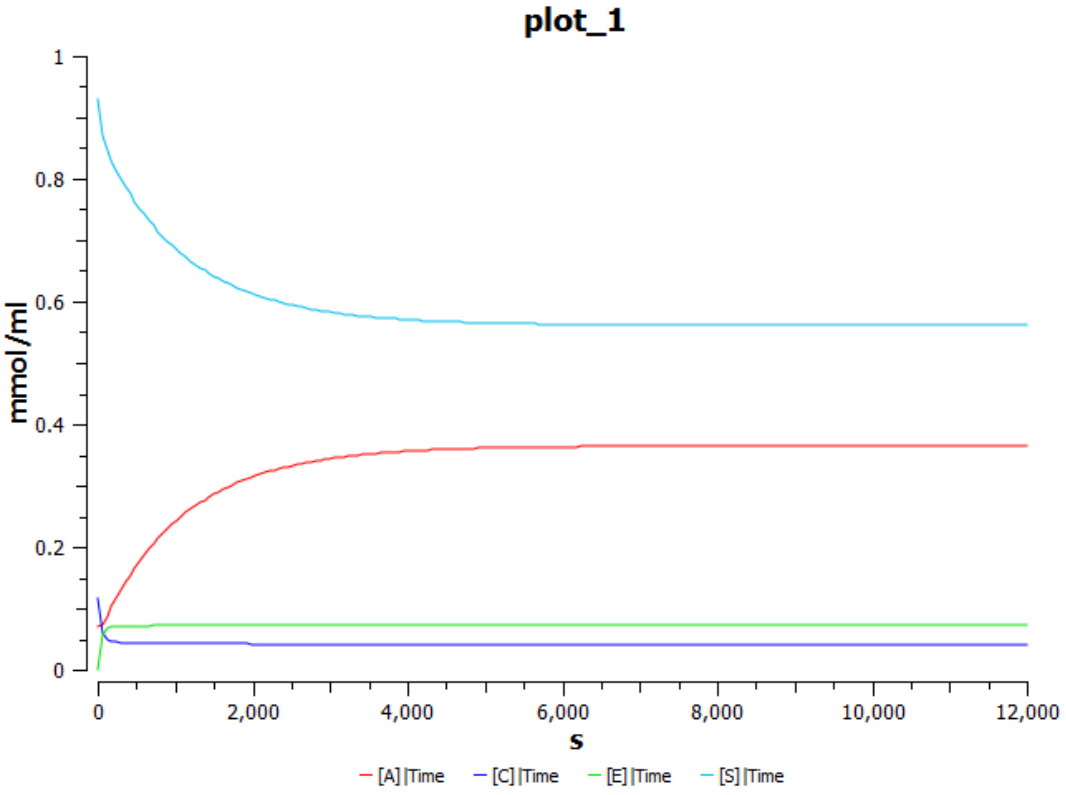

7.2. Selective (s=39) epimerization of (2*R*,3*S*)-2-methyl-4-nitro-3-phenylbutanal

To adjust the data to the experimental results the selectivity has to be 39 (for the k_s value estimated previously or higher for a higher k_s):

$$k_{-s} = 39\, k_{-a}$$

So, all the kinetic constants are:

$$k_s = 1.00\ \mathrm{M^{-1}min^{-1}};\ k_{-s} = \frac{k_s}{3.19} = 0.31\ \mathrm{M^{-1}min^{-1}}$$

$$k_a = \frac{4.91}{3.19 \cdot 39} k_s = 0.039\ \mathrm{M^{-1}min^{-1}};\ k_{-a} = \frac{1}{3.19 \cdot 39} k_s = 12.23\ \mathrm{M^{-1}min^{-1}}$$

And the results show that the equilibration takes 2500 min.

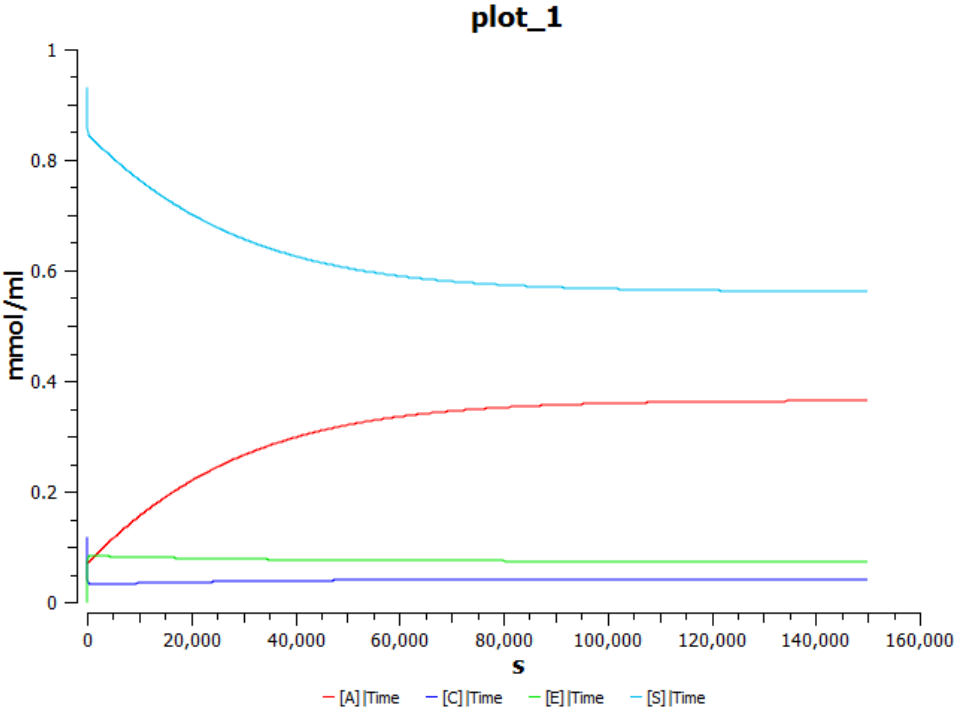

These modeled data match perfectly the experimental data:

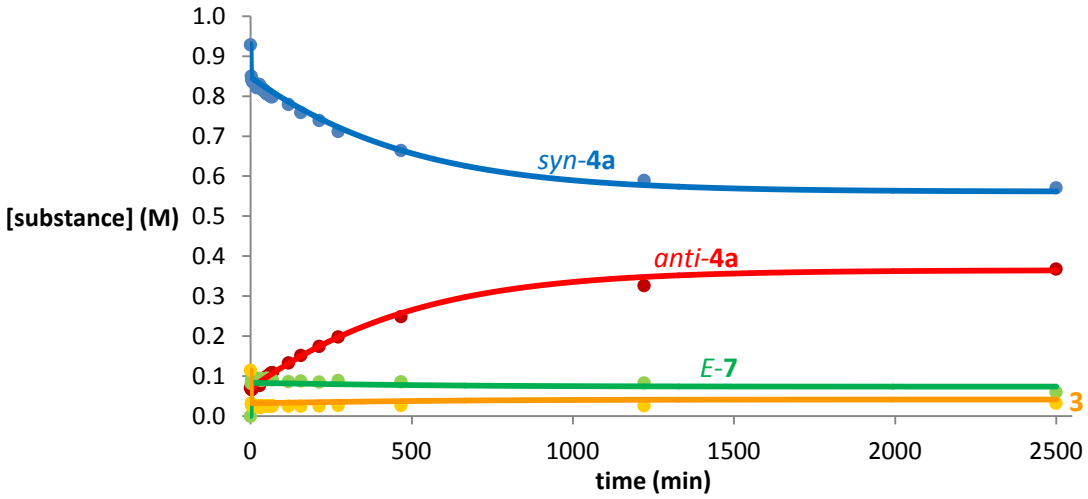

8. Definition of the Curtin-Hammett principle

IUPAC[4] definition of the Curtin-Hammett principle (underlining added):

Curtin–Hammett principle

In a *chemical reaction* that yields one product (X) from one conformational isomer (A′) and a different product (Y) from another conformational isomer (A″) (and provided these two isomers are rapidly interconvertible relative to the rate of product formation, whereas the products do not undergo interconversion) the product composition is not in direct proportion to the relative concentrations of the conformational isomers in the *substrate*; it is controlled only by the difference in standard free energies (DD$G^{‡}$) of the respective *transition states.*

It is also true that the product composition is formally related to the relative concentrations of the conformational isomers A′ and A″ (*i.e.* the conformational equilibrium constant) and the respective rate constants of their reactions.

Consider the case described of the Curtin-Hammett relationship between conformers A' and A" and products X and Y, shown in the diagram shown below. The **first paragraph** of the IUPAC definition gives the product ratio in terms of the difference in transition state energies. The **second paragraph** of the IUPAC definition gives the product ratio in terms of the relative intermediate concentrations and the respective rate constants:

$$\frac{[Y]}{[X]} = \exp\left(\frac{-\Delta\Delta G^{‡}}{RT}\right) \qquad \frac{[Y]}{[X]} = \frac{[A'']}{[A']} \cdot \frac{k''}{k'}$$

from relative stabilities (thermodynamics) — *from realtive reactivities (kinetics)*

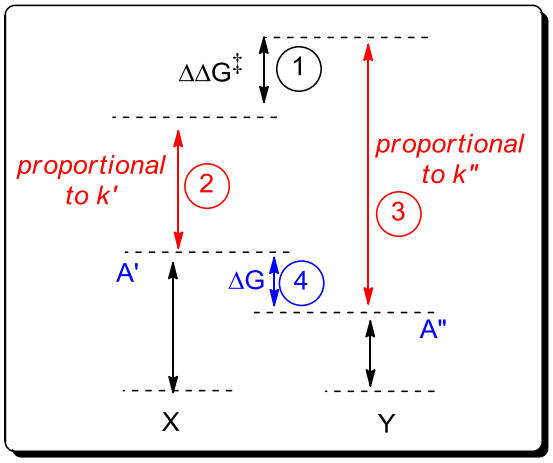

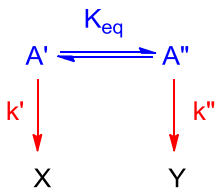

$\Delta G = -RT \ln K_{eq}$

$K_{eq} = [A'']/[A']$

1 = 3 - 2 - 4

The magnitude of the $\Delta\Delta G^{\ddagger}$ barrier (black arrow, **1**) is obtained by taking the energy difference for pathway k" (red arrow, **3**) minus that for pathway k' (red arrow, **2**) *AND* minus that for the thermodynamic difference between intermediate energies (blue arrow, **4**). It is this last contribution, the difference in the energy minima giving the intermediate stabilities, that is referred to in the second paragraph of the definition.

This shows that the product ratio (and thus the relative barrier height of the TS) is made up of two components:

1. the ratio of the small k values (k' and k"), which indicate the relative ***height*** of the energy maxima from the point of the intermediates (A' and A", respectively).
2. the relative ***depth*** of the energy minima for the two intermediates, which is given by the capital K_{eq}. This equilibrium constant corresponds to the relative stability, or concentration of the two intermediates.

It is clear that ***both*** factors affect the ultimate $\Delta\Delta G^{\ddagger}$. It is demonstrates that the ultimate product ratio may be controlled mostly by one, or by the other, or by contributions from both factors.

It is also clear that in any particular case the kinetic and thermodynamic contributions may either augment one another (as in "lock-and-key" kinetics, where the most stable intermediate is most reactive), or they may act in opposite manners ((such as the classic Landis-Halpern case, where the more stable intermediate reacted more slowly). Because kinetics and thermodynamics have no predictive relationship to one another, the relative contributions can't be predicted a priori.

Thus the Curtin-Hammett principle does in fact depend on the relative stability of intermediates. In general, the dependence is *not in a proportional or predictive manner*.

To summarize, as mentioned in point a) above, ***the transition state described by Model II is in fact not the appropriate TS in the two examples we discuss***. Model **II** looks at the ***wrong step*** for rationalizing enantioselectivity in these cases! The $\Delta\Delta G^{\ddagger}$ described by Model **II**, enamine attack on nitrostyrene (k_2/k_2') does ***not*** dictate the product ratio for the system following Pathway B, as was demonstrated in the Equation in Figure 6c of the manuscript.

Our work demonstrates that a rationalization of stereochemical outcome needs to compare:

- **how high are the peaks** (individual transition states), and
- **how deep are the valleys** (stability of intermediates)

but above all, we need to be sure that we have ascertained:

- **what is the relevant transition state**, i.e., is the transition state under consideration in fact the step which dictates the stereochemical outcome?

9. Kinetic of chlorination reactions

Measurements were performed using an Omnical Insight reaction calorimeter, which allows continuous monitoring of the instantaneous heat absorbed or released by a chemical reaction occurring in the vessel. The sample vessel is a 16 mL septum-cap vial equipped with a magnetic stirring bar. The system operates as a differential scanning calorimeter by comparing the heat released or consumed in a sample vessel with that from a reference compartment at intervals of 3 seconds over the course of the reaction.

The reactions were set up from common stock solutions:

Stock solution A: 1.1520 g of, total volume of 1 mL of $CHCl_3$.
Stock solution B: 500 mg of (*S*)-α,α-diphenyl-2-pyrrolidinemethanol trimethylsilyl, total volume of 1 mL of $CHCl_3$.
Stock solution C: 90 mg of acetic acid, total volume of 10 mL of $CHCl_3$.

Reaction with NCS (2b): 260 mg of NCS + 2.80 mL of SL A + 200 µL of SL C, then injection of 100 µL of SL B.

Reaction with PhthNCl (2c): 345 mg of *N*-chlorophthalimide + 2.80 mL of SL A + 200 µL of SL C, then injection of 100 µL of SL B.

The results are summarized in the following figures.

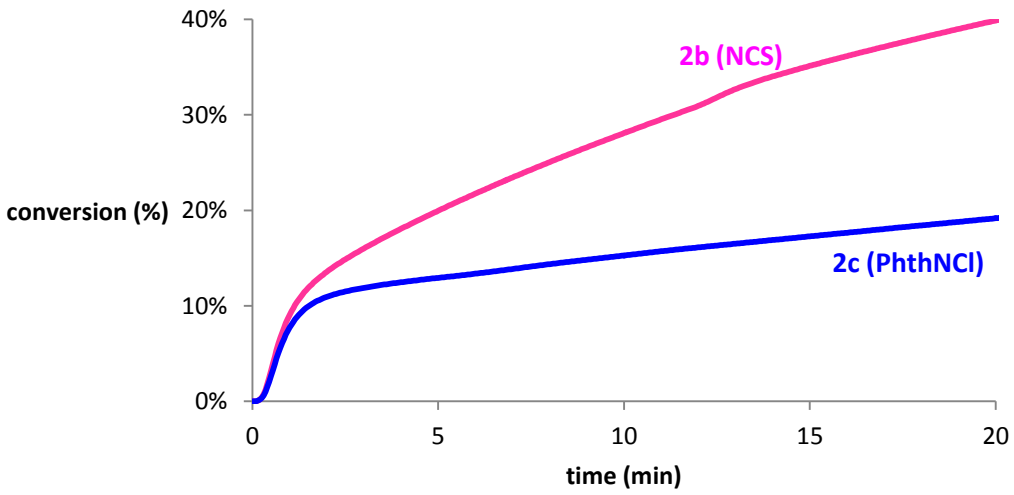

Figure 8. Kinetics of the chlorination reaction of 2b and 2c catalyzed by 3 at –11.8 °C.

10. NMR studies of the intermediates in chlorination reactions

A premixed solution of isovaleraldehyde (0.39 mmol) and catalyst (0.03 mmol) in $CDCl_3$ were added to NCS or PhthNCl (0.30 mmol) in a NMR tube at room temperature and then introduced in the NMR pre-stabilized at –54 °C.

The complete characterization of the diastereomeric species observed was done for (*S*)-α,α-bis[3,5-bis(trifluoromethyl)phenyl]-2-pyrrolidinemethanol because is the slower catalyst. The other ones were assigned by comparison with the first one due to the similarity of the systems.

10.1. Intermediate from: **1c** + **2b** + **catalyst 11**

Over the reaction at room temperature the catalyst is totally captured as a species that looks as a single diastereoisomer, but at temperatures below –30 °C it is possible to differentiate two diastereoisomers in equilibrium (as the EXSY cross-peaks certify).

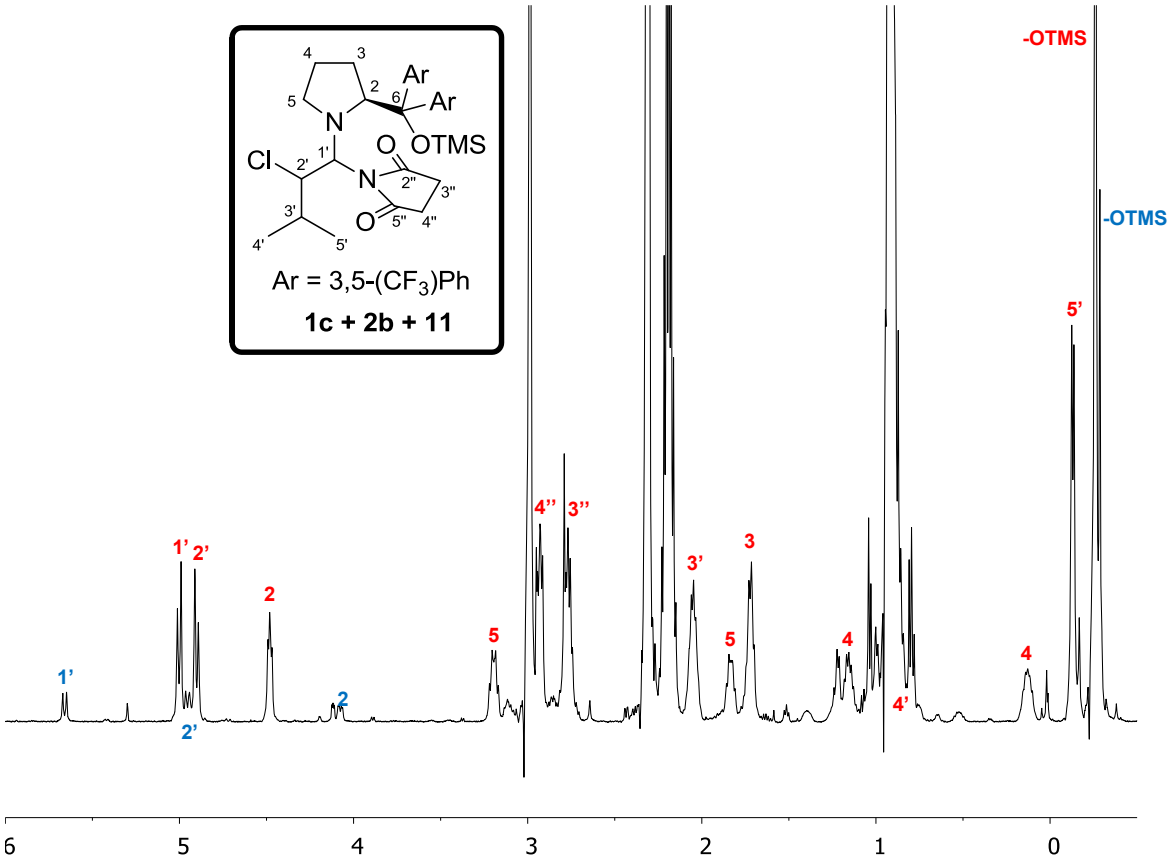

Figure 9. ^{1}H-NMR of the intermediate from 1c + 2b + catalyst 11 at –54 °C.

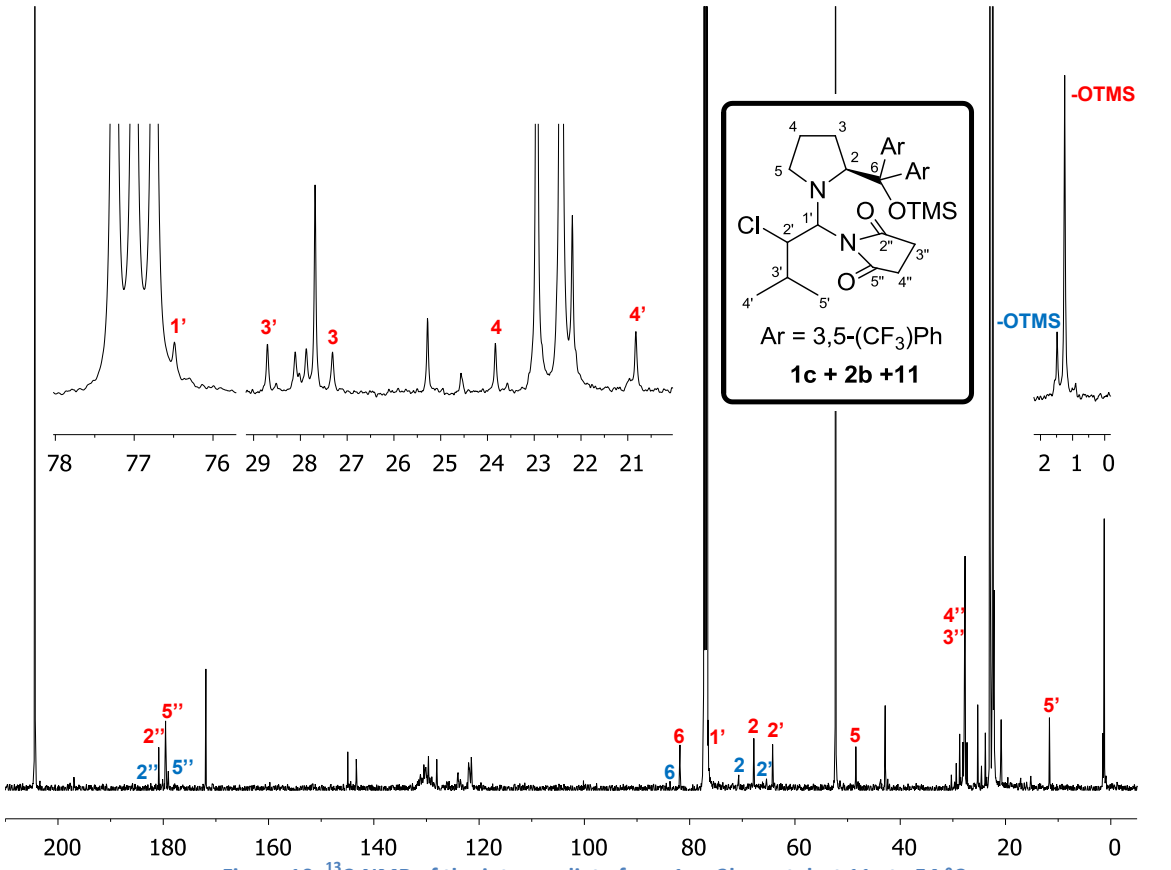

Figure 10. ^{13}C-NMR of the intermediate from 1c + 2b + catalyst 11 at –54 °C.

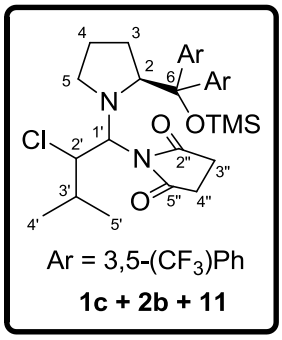

1-(1-((*S*)-2-(bis(3,5-bis(trifluoromethyl)phenyl)((trimethylsilyl)oxy)-methyl)pyrrolidin-1-yl)-2-chloro-3-methylbutyl)pyrrolidine-2,5-dione: major diasteroisomer: ^{1}H-NMR (500 MHz, $CDCl_3$) δ –0.26 (s, 9H; OTMS), –0.13 (d, 3H, *J* = 6.6; C(5')H), 0.07–0.19 (m, 1 H; C(4)H), 0.88–0.93 (3H; C(4')H), 1.11–1.19 (m, 1 H; C(4)H), 1.67–1.77 (m, 2 H; C(3)H), 1.79–1.88 (m, 1 H; C(5)H), 1.99–2.10 (m, 1 H; C(3')H), 2.72–2.82 (m, 2 H; C(3")/4")H), 2.89–2.96 (m, 2 H; C(3")/4")H), 3.15–3.25 (m, 1 H; C(5)H), 4.48 (dd, 1 H, *J* = 5.0, *J* = 7.3; C(2)H), 4.90 (dd, 1 H, *J* = 10.5, *J* = 1.7; C(2')H), 5.00 (d, 1 H, *J* = 10.5; C(1')H), 7.20–7.31 (br, 1 H; Ar), 7.58–7.68 (br, 1 H; Ar), 7.88–7.96 (br, 3 H; Ar), 8.11–8.19 (br, 1 H; Ar); **^{13}C-NMR** (125.7 MHz, $CDCl_3$) δ 180.9 (C2"), 179.5 (C5"), 81.9 (C6), 76.5 (C1'), 67.8 (C2), 64.3 (C2'), 48.4 (C5), 88.7 (C3'), 27.3 (C3), 23.8 (C4), 20.8 (C4'), 11.7 (C5'), 1.3 (OTMS). **Minor diasteroisomer: ^{1}H-NMR** (500 MHz, $CDCl_3$) δ –0.29 (s, 9H; OTMS), 4.08 (dd, 1 H, *J* = 10.1, *J* = 3.7; C(2)H), 4.95 (dd, 1 H, *J* = 9.0, *J* = 2.0; C(2')H), 5.66 (d, 1 H, *J* = 10.8; C(1')H); **^{13}C-NMR** (125.7 MHz, $CDCl_3$) δ 180.1 (C2"), 179.0 (C5"), 83.7 (C6), 70.7 (C2), 65.4 (C2'), 1.5 (OTMS).

The assignment of the molecule is based on the two dimensional experiments shown below.

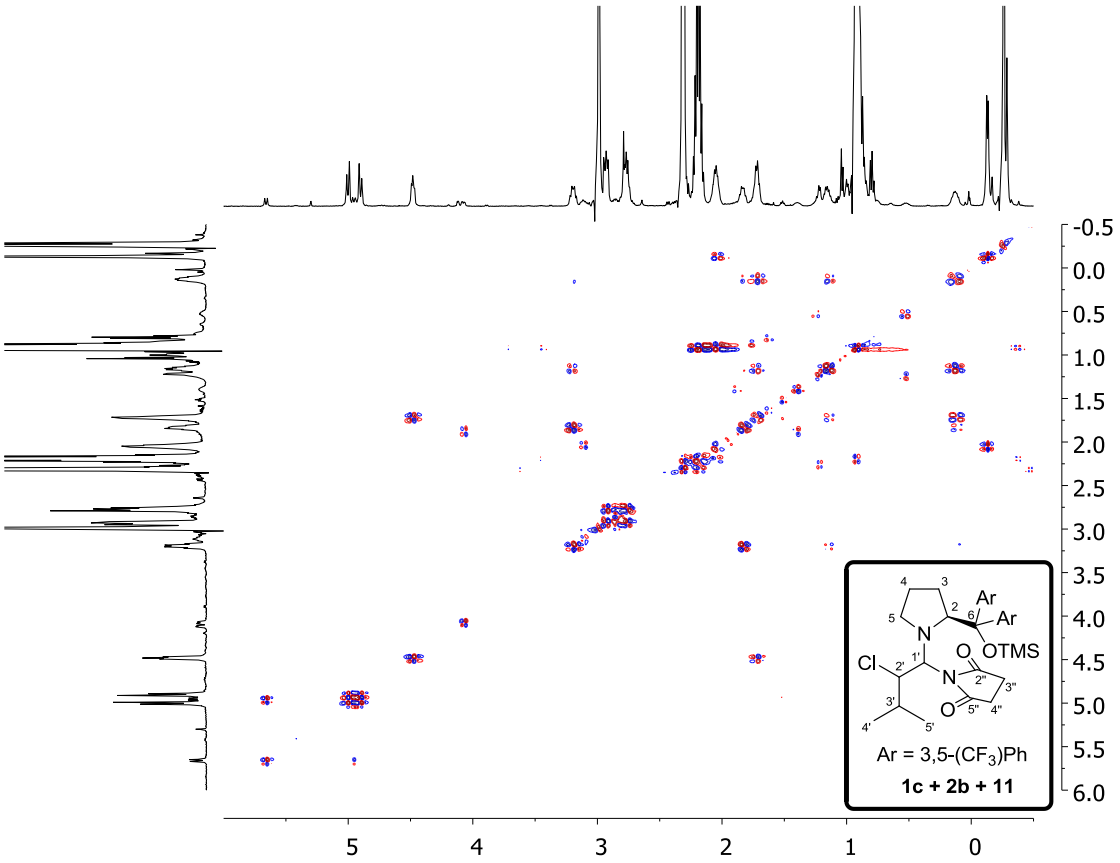

Figure 11. COSY of intermediates from 1c + 2b + catalyst 11 at –54 °C.

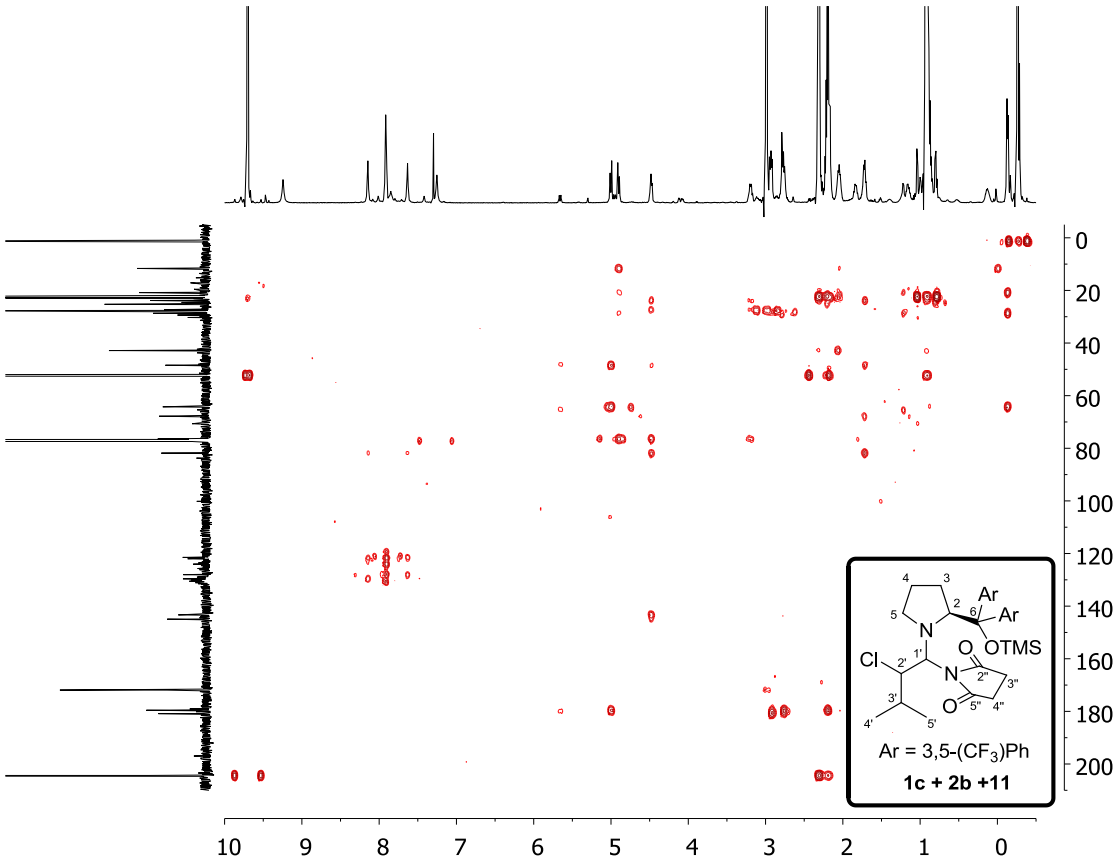

Figure 12. HMBC of intermediates from 1c + 2b + catalyst 11 at –54 °C.

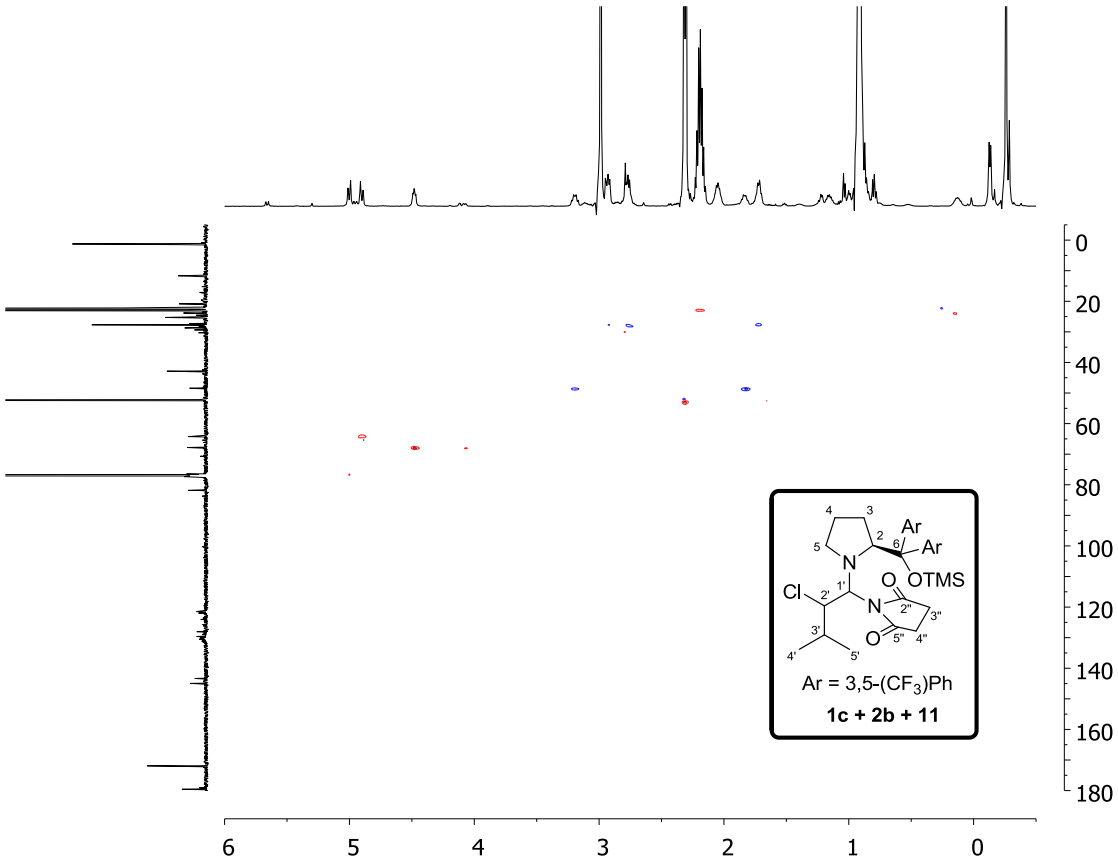

Figure 13. HSQC of intermediates from 1c + 2b + catalyst 11 at –54 °C.

The spectra at different temperatures show the coalescence of the signals of two diastereoisomers in equilibrium. At room temperature, it looks like there is only one species, but at temperatures below –30 °C the rates of equilibration are slower and two different diastereoisomers are observed.

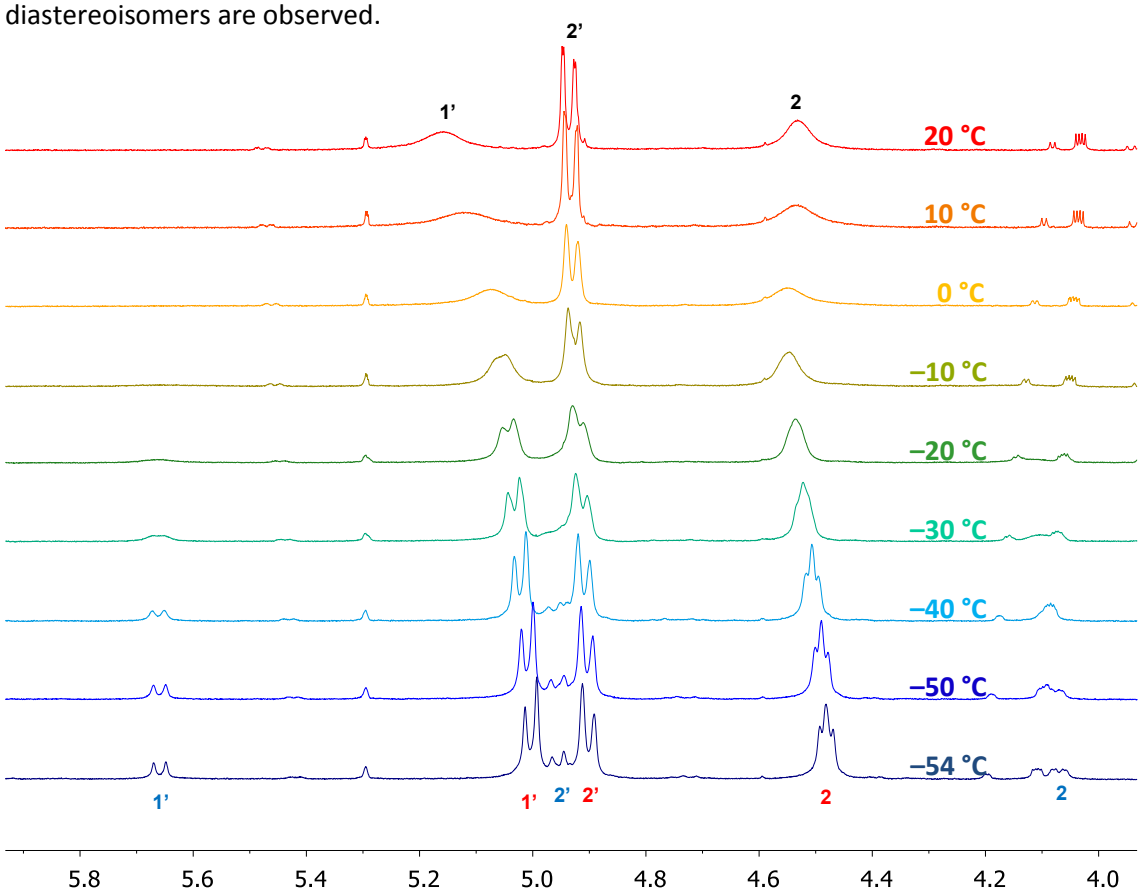

Figure 14. Coalescence of ^{1}H-NMR signals of diastereomeric intermediates from 1c + 2b + 11 at different temperatures.

In addition, the EXSY cross-peaks at –54 °C show that the two diastereoisomers are in equilibrium.

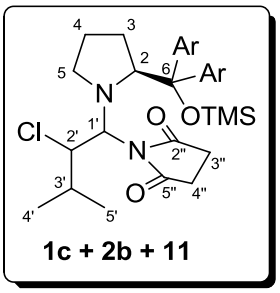

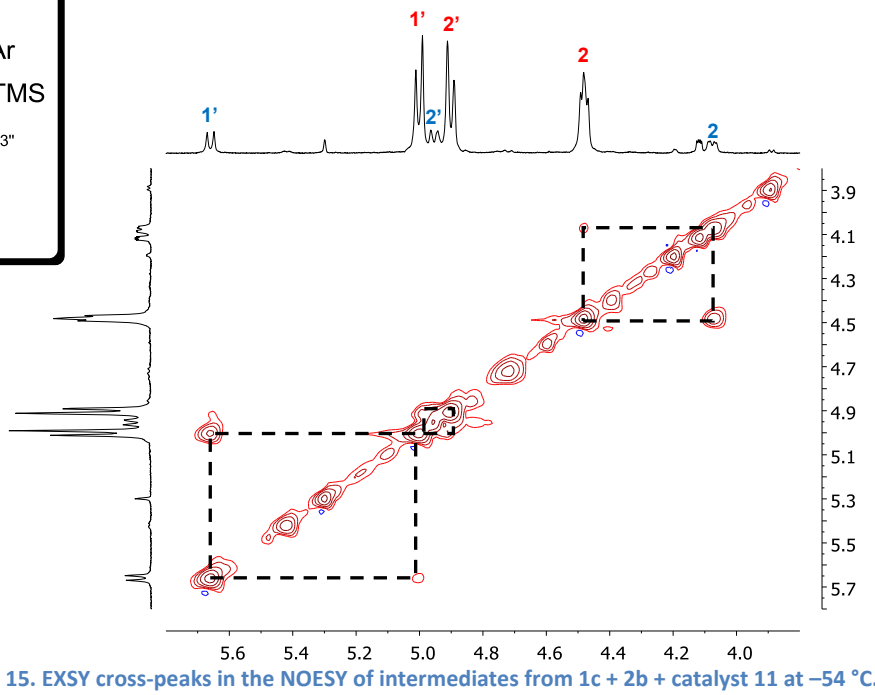

Figure 15. EXSY cross-peaks in the NOESY of intermediates from 1c + 2b + catalyst 11 at –54 °C.

entry	catalyst	Cl-Y	diastereomeric ratio of intermediates (**NMR**)	enantiomeric ratio of product (**Chiral-GC**)
2	**11**	**2b**	**16:84**	**16:84**

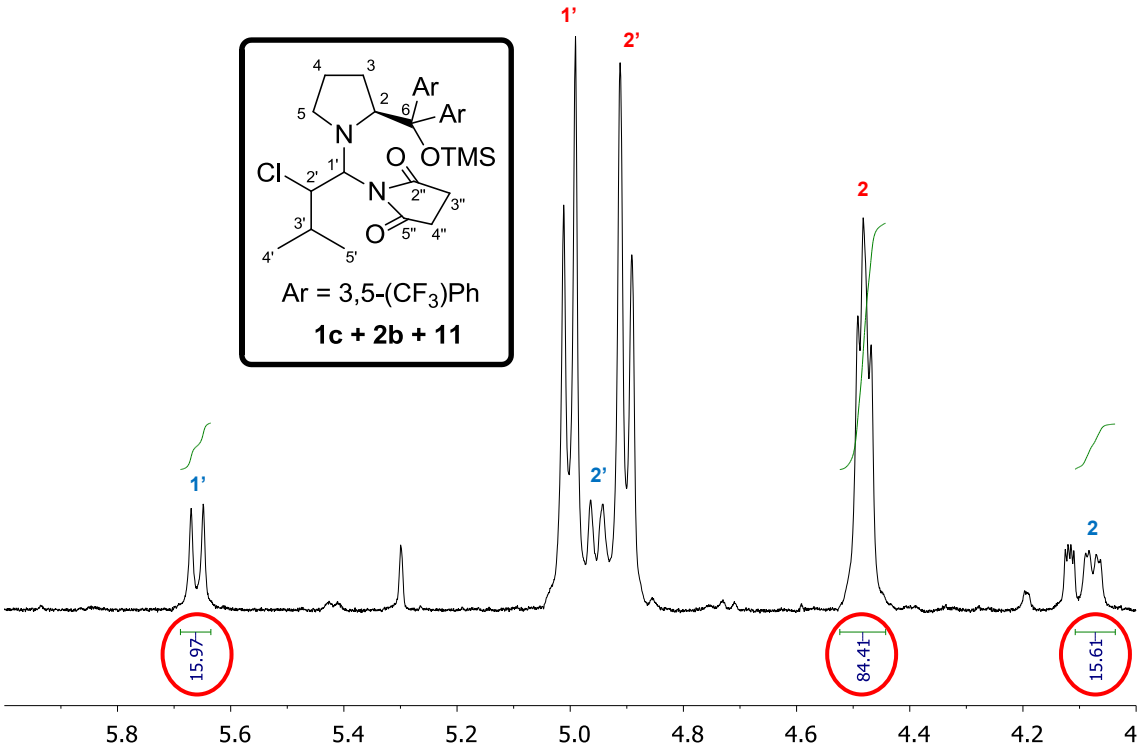

Figure 16. ^{1}H-NMR of the intermediate from 1c + 2b + catalyst 11 at –54 °C (Table 1, entry 2).

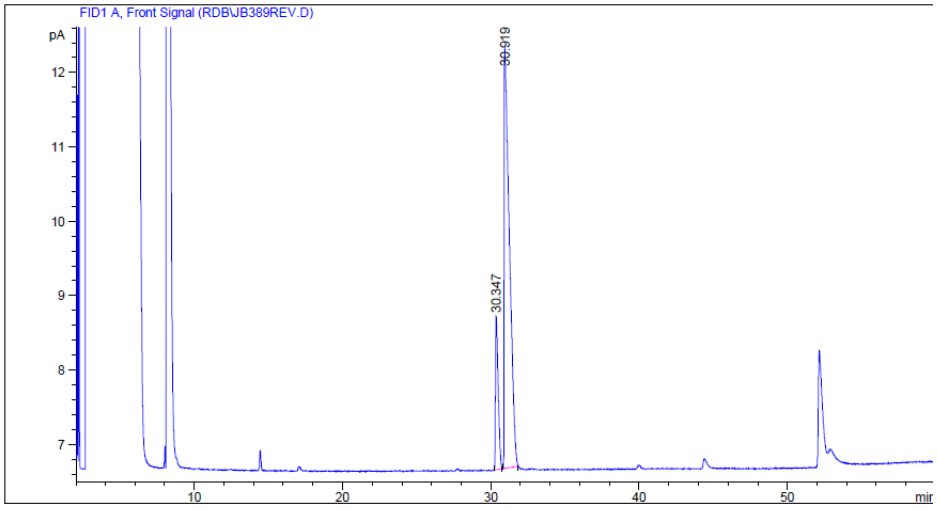


```
=====================================================================
                      Area Percent Report
=====================================================================

Sorted By             :      Signal
Multiplier:                   :      1.0000
Dilution:                     :      1.0000
Use Multiplier & Dilution Factor with ISTDs


Signal 1: FID1 A, Front Signal

Peak RetTime Type  Width     Area      Height     Area
  #   [min]        [min]   [pA*s]      [pA]        %
----|-------|----|-------|----------|----------|--------|
   1  30.347 BB    0.1630   25.80766    2.06209 15.82733
   2  30.919 BB    0.2944  137.24995    5.68934 84.17267
```

Figure 17. Chiral GC of the product of reaction of 1c and 2b, catalyzed by 11 from 0 °C to rt (Table 1, entry 2).

10.2. Intermediate from: 1c + 2b + catalyst 3

The spectra at different temperatures show the coalescence of the signals of two diastereoisomers in equilibrium. At room temperature, it looks like there is only one species, but at temperatures below –30 °C the rates of equilibration are slower and two different diastereoisomers are observed.

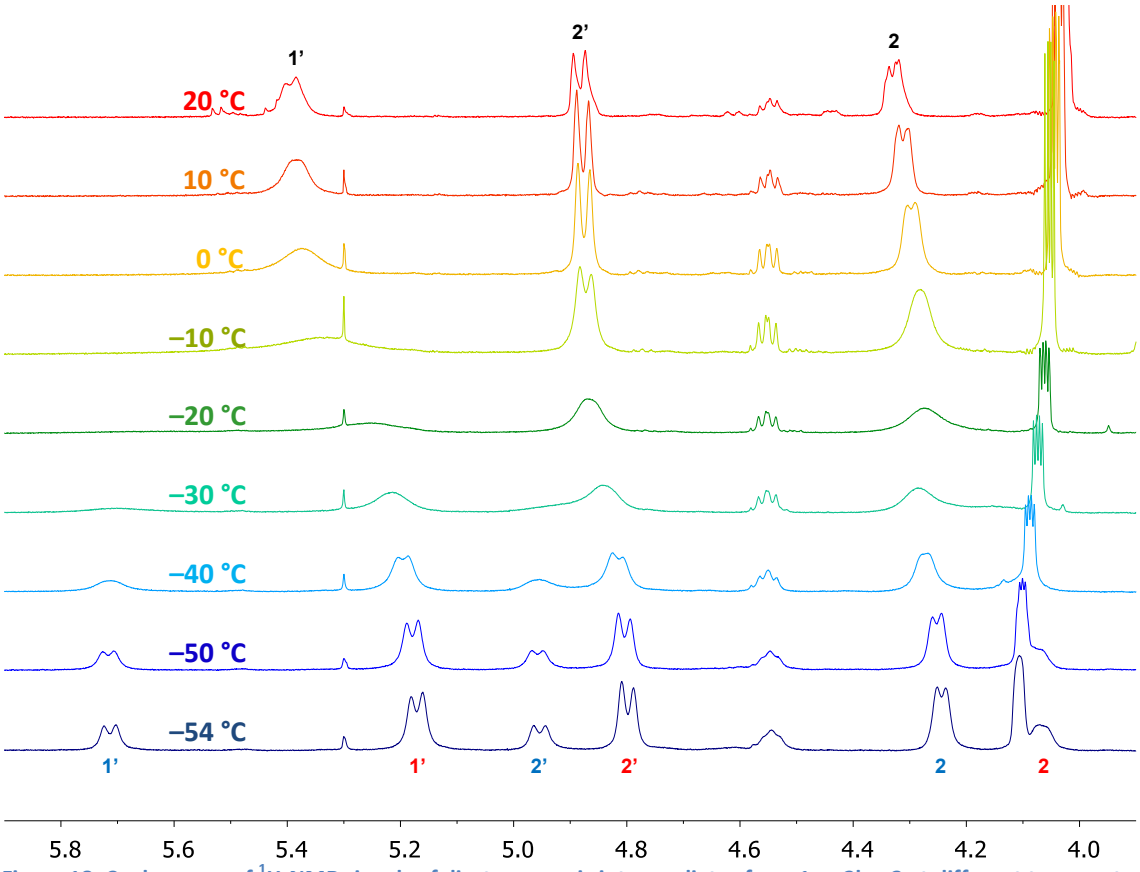

Figure 18. Coalescence of ^{1}H-NMR signals of diastereomeric intermediates from 1c + 2b + 3 at different temperatures.

In addition, the EXSY cross-peaks at –54 °C show that the two diastereoisomers are in equilibrium.

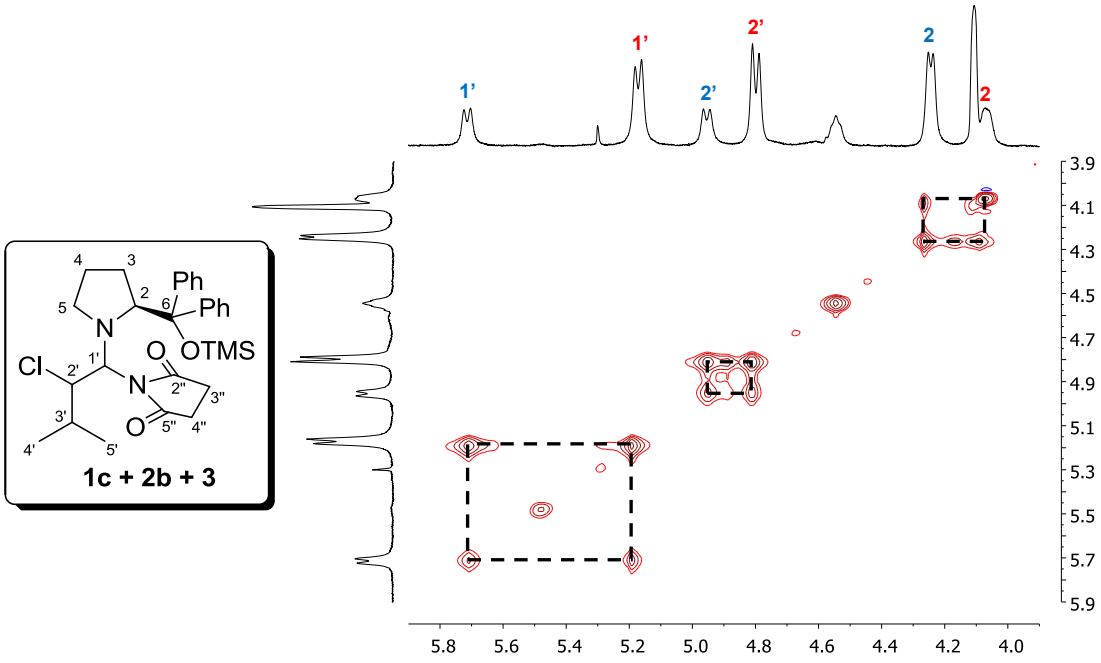

Figure 19. EXSY cross-peaks in the NOESY of intermediates from 1c + 2b + catalyst 3 at –54 °C.

entry	catalyst	Cl-Y	diastereomeric ratio of intermediates (**NMR**)	enantiomeric ratio of product (**Chiral-GC**)
1	**3**	**2b**	**30:70**	**29:71**

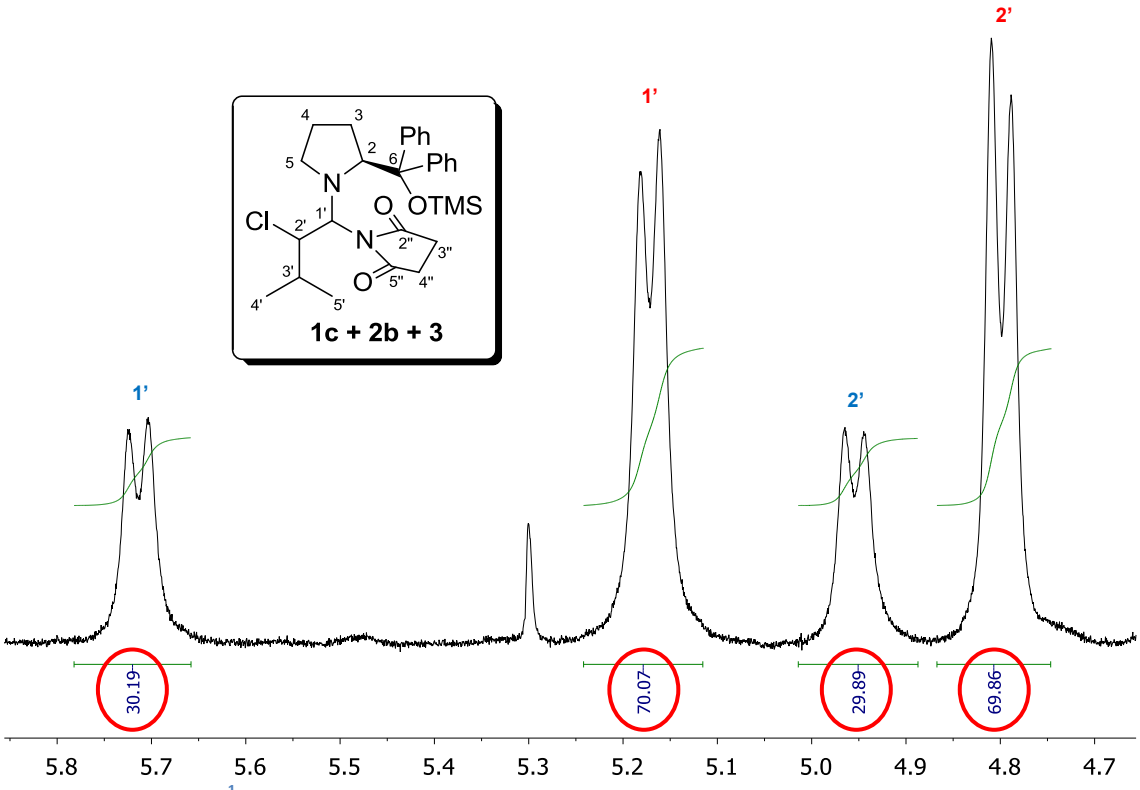

Figure 20. ^{1}H-NMR of the intermediate from 1c + 2b + catalyst 3 at –54 °C (Table 1, entry 1).

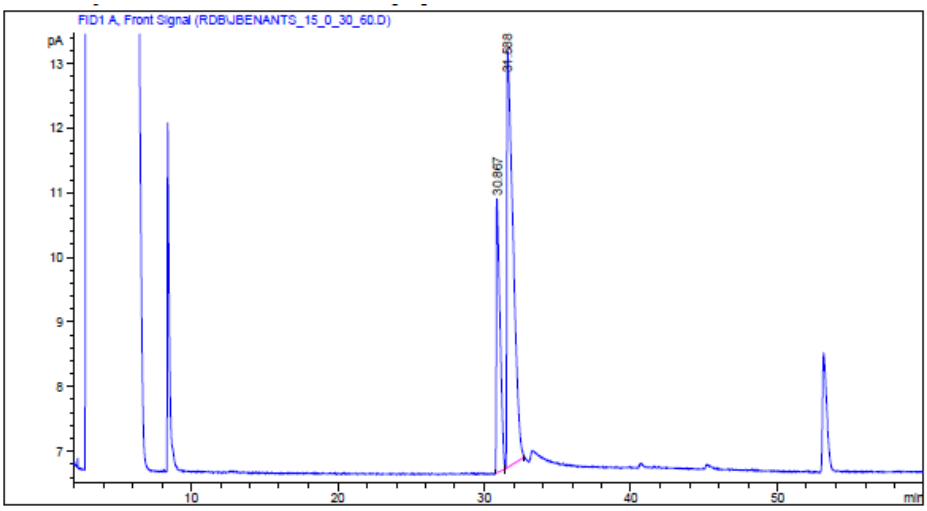


```
=====================================================================
                    Area Percent Report
=====================================================================

Sorted By             :      Signal
Multiplier:                   :      1.0000
Dilution:                     :      1.0000
Use Multiplier & Dilution Factor with ISTDs


Signal 1: FID1 A, Front Signal

Peak RetTime Type  Width     Area      Height     Area
  #   [min]        [min]   [pA*s]      [pA]        %
----|-------|----|-------|----------|----------|--------|
   1  30.867 BV    0.2283   75.76936    4.24430 28.58682
   2  31.588 VB    0.3462  189.28058    6.45225 71.41318
```

Figure 21. Chiral GC of the product of reaction between 1c and 2b, catalyzed by 3 from 0 °C to rt (Table 1, entry 1).

10.3. Intermediate from: 1c + 2b + catalyst 12

In this case only one diastereoisomer was detected even at low temperatures (–54 °C).

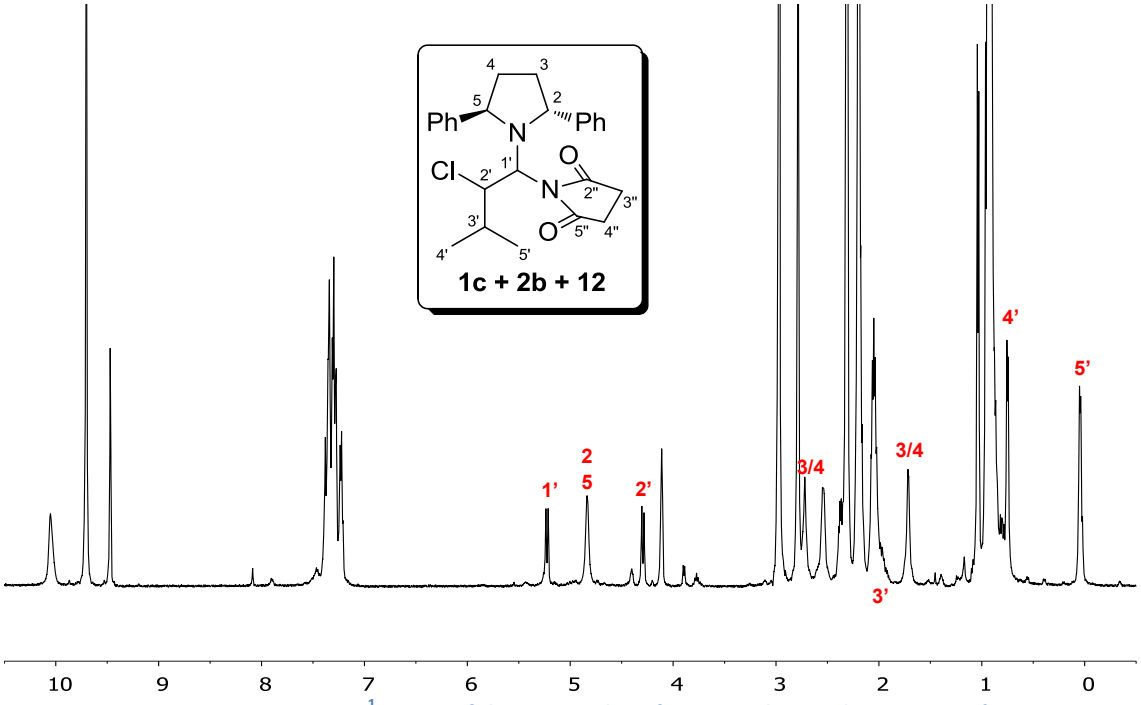

Figure 22. ^{1}H-NMR of the intermediate from 1c + 2b + catalyst 12 at –54 °C.

In addition, there is not any shift of the signals corresponding to the chlorinated intermediate at different temperatures (observed previously for cat **3** and **11** due to the coalescence effect).

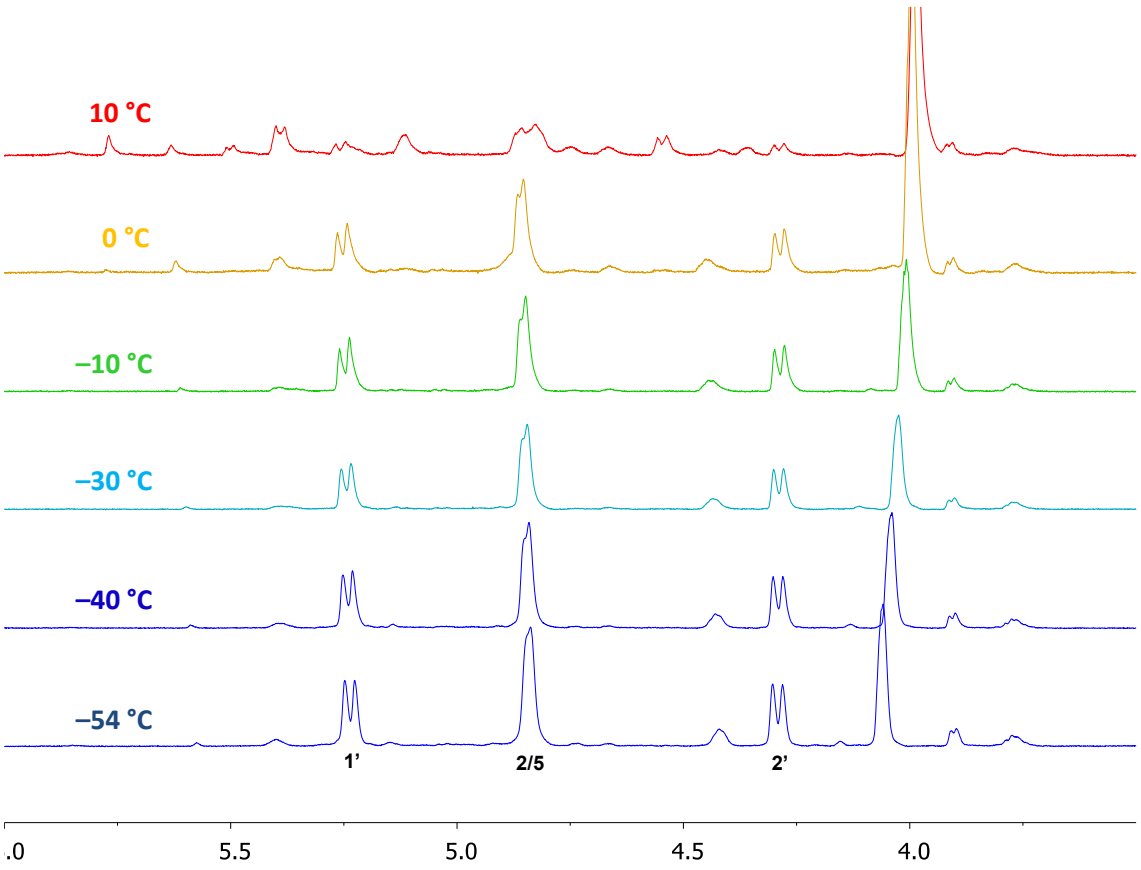

Figure 23. ^{1}H-NMR signals of intermediate from 1c + 2b + 12 at different temperatures without changes in shifts.

10.4. Intermediate from: 1c + 2c + catalyst 11

The spectra at different temperatures show the coalescence of the signals of two diastereoisomers in equilibrium. At room temperature, it looks like there is only one species, but at temperatures below –10 °C the rates of equilibration are slower and two different diastereoisomers are observed.

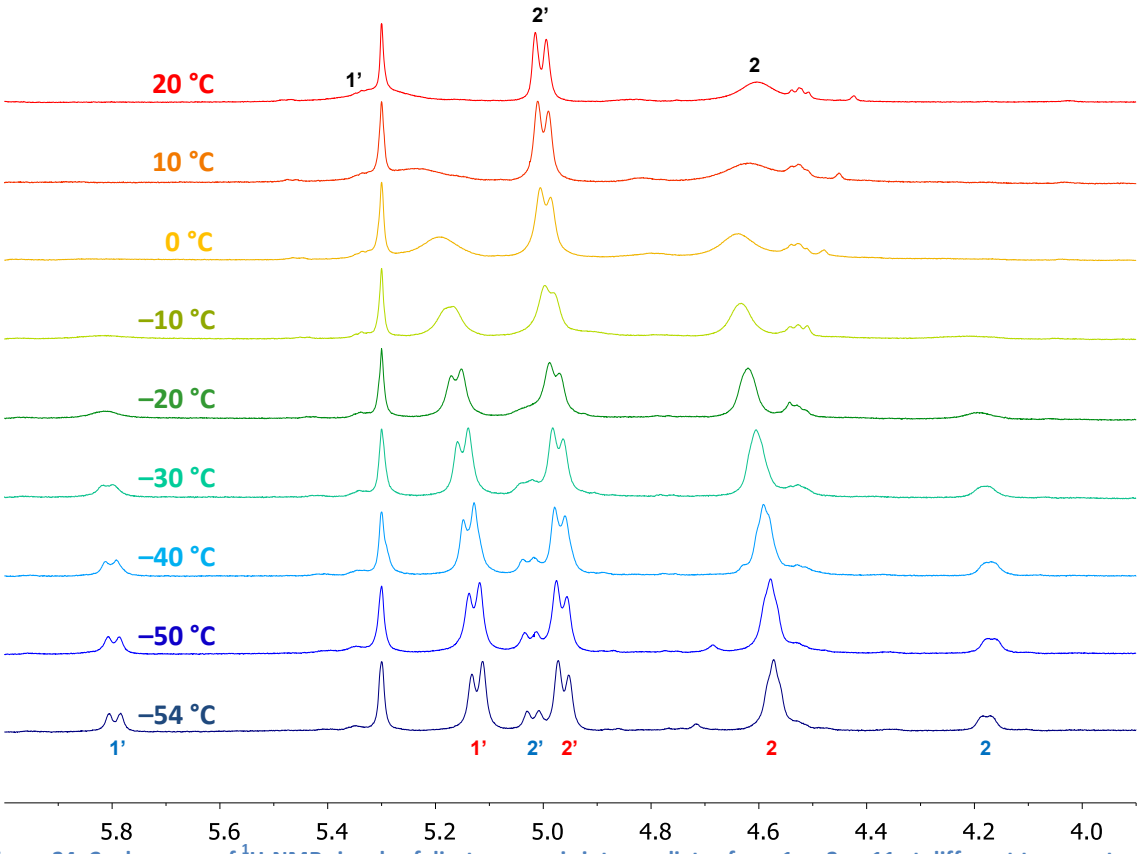

Figure 24. Coalescence of ^{1}H-NMR signals of diastereomeric intermediates from 1c + 2c + 11 at different temperatures.

In addition, the EXSY cross-peaks at –54 °C show that the two diastereoisomers are in equilibrium.

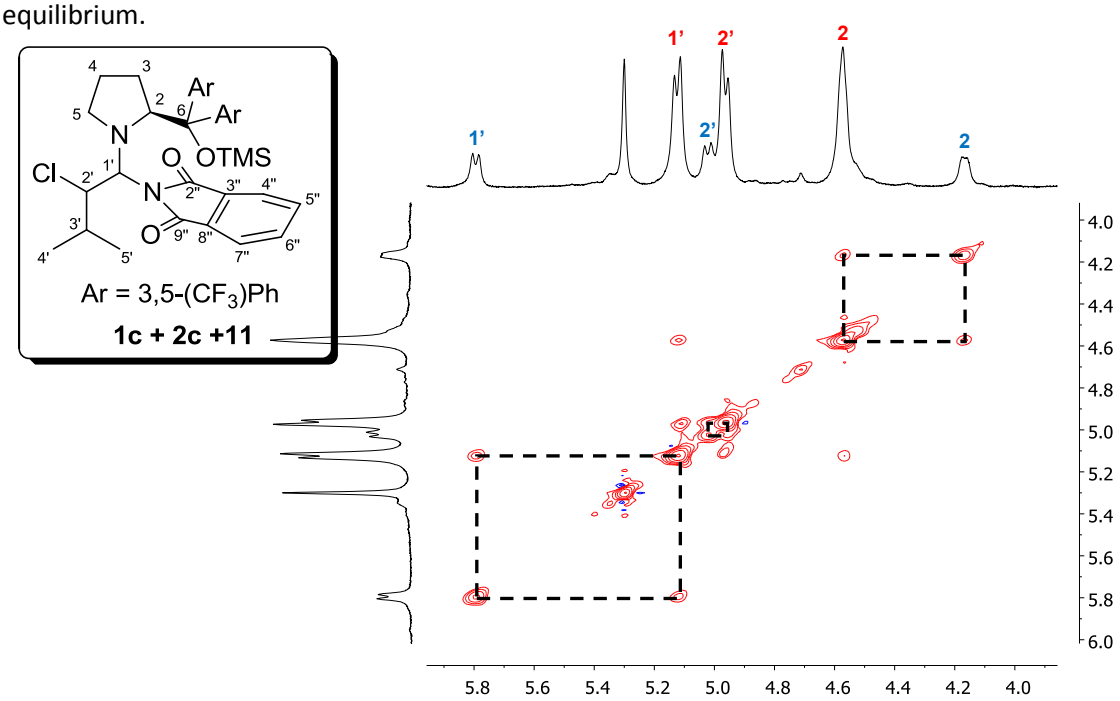

Figure 25. EXSY cross-peaks in the NOESY of intermediates from 1c + 2c + catalyst 11 at –54 °C.

entry	catalyst	Cl-Y	diastereomeric ratio of intermediates (**NMR**)	enantiomeric ratio of product (**Chiral-GC**)
5	**11**	**2c**	**21:79**	**21:79**

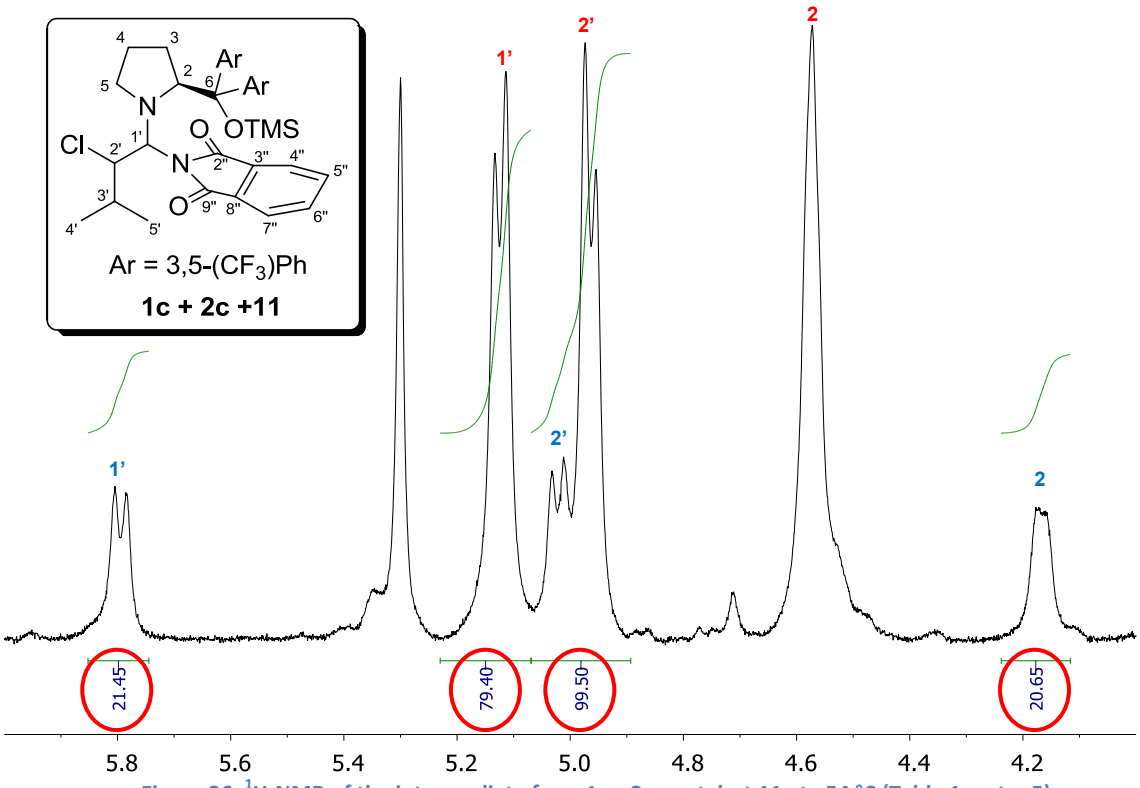

Figure 26. ^{1}H-NMR of the intermediate from 1c + 2c + catalyst 11 at –54 °C (Table 1, entry 5).

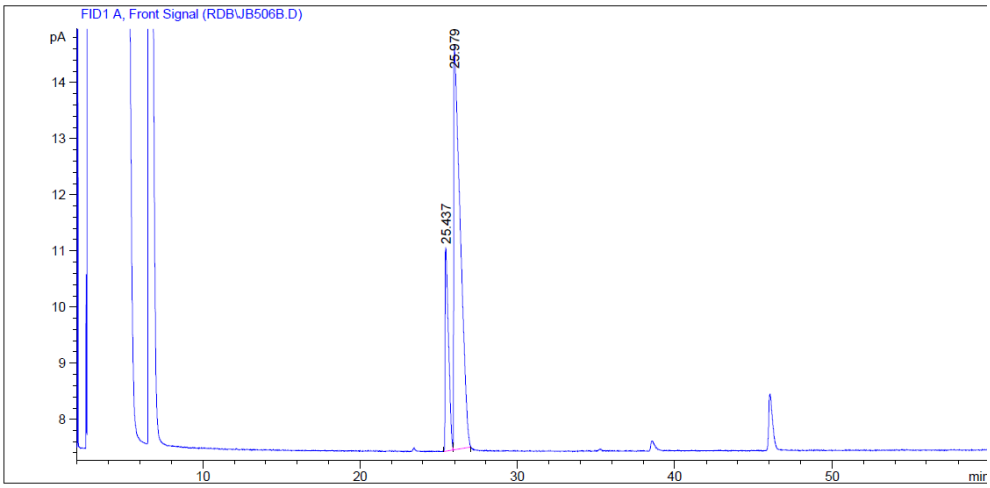


```
=====================================================================
                      Area Percent Report
=====================================================================

Sorted By             :      Signal
Multiplier:                   :      1.0000
Dilution:                     :      1.0000
Use Multiplier & Dilution Factor with ISTDs


Signal 1: FID1 A, Front Signal

Peak RetTime Type  Width     Area      Height     Area
  #   [min]        [min]    [pA*s]     [pA]        %
----|-------|----|-------|----------|----------|--------|
   1  25.437 BV    0.1928   53.83269    3.63385 20.77816
   2  25.979 VB    0.3451  205.25034    7.20977 79.22184
```

Figure 27. Chiral GC of the product of reaction of 1c and 2c, catalyzed by 11 from 0 °C to rt (Table 1, entry 5).

10.5. Intermediate from: 1c + 2c + catalyst 3

The spectra at different temperatures show the coalescence of the signals of two diastereoisomers in equilibrium. At room temperature, it looks like there is only one species, but at temperatures below –20 °C the rates of equilibration are slower and two different diastereoisomers are observed.

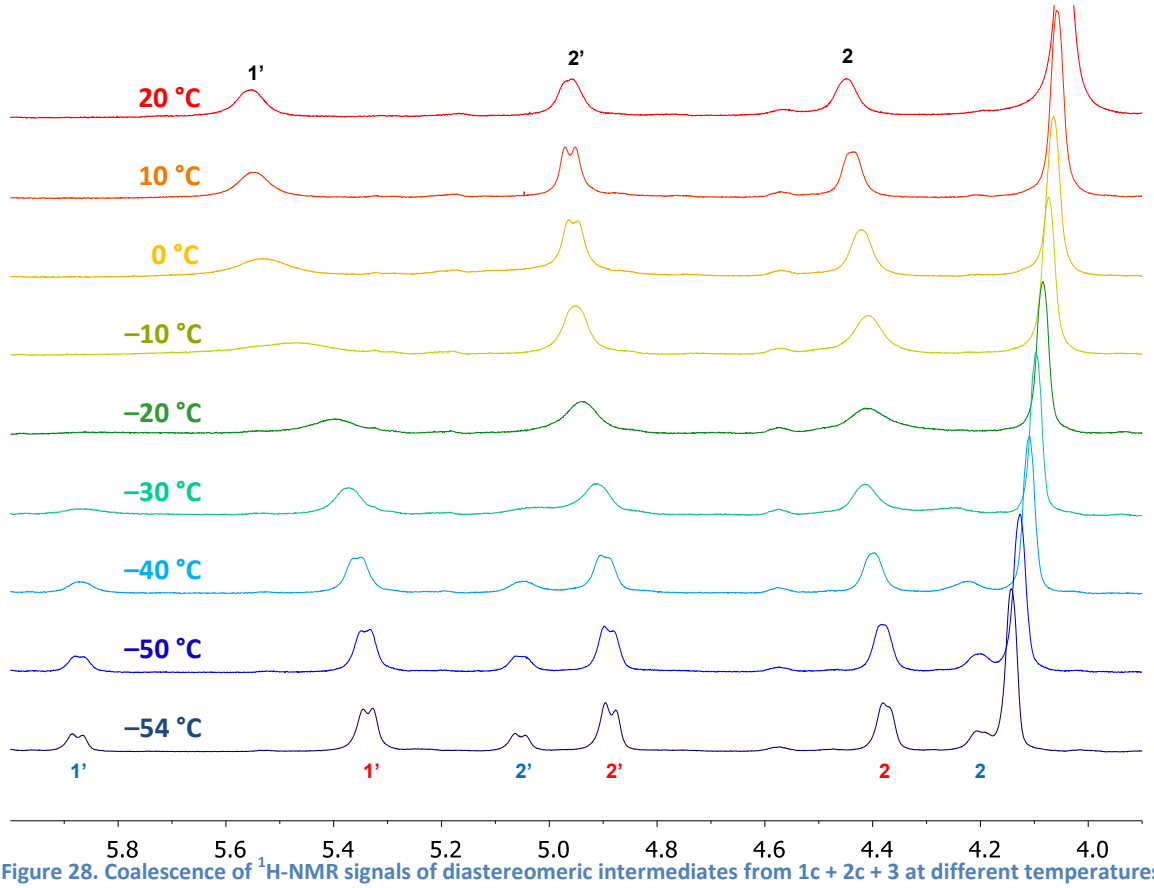

Figure 28. Coalescence of ^{1}H-NMR signals of diastereomeric intermediates from 1c + 2c + 3 at different temperatures.

In addition, the EXSY cross-peaks at –54 °C show that the two diastereoisomers are in equilibrium.

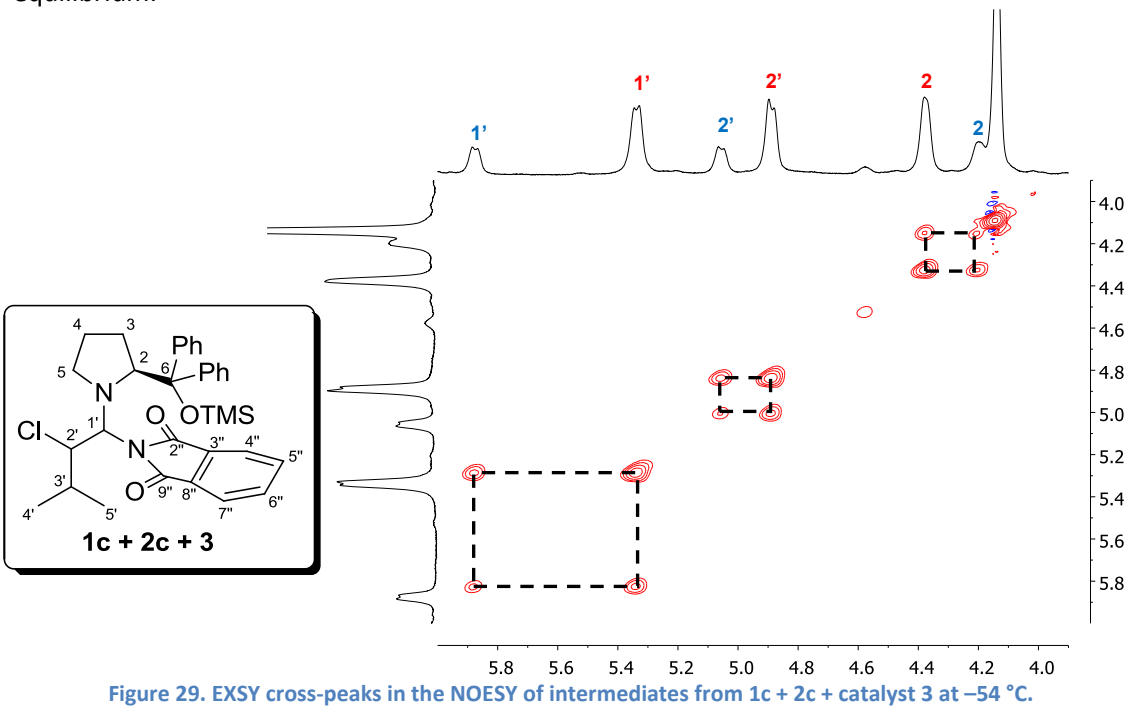

Figure 29. EXSY cross-peaks in the NOESY of intermediates from 1c + 2c + catalyst 3 at –54 °C.

entry	catalyst	Cl-Y	diastereomeric ratio of intermediates (**NMR**)	enantiomeric ratio of product (**Chiral-GC**)
4	**3**	**2c**	**26:74**	**23:77**

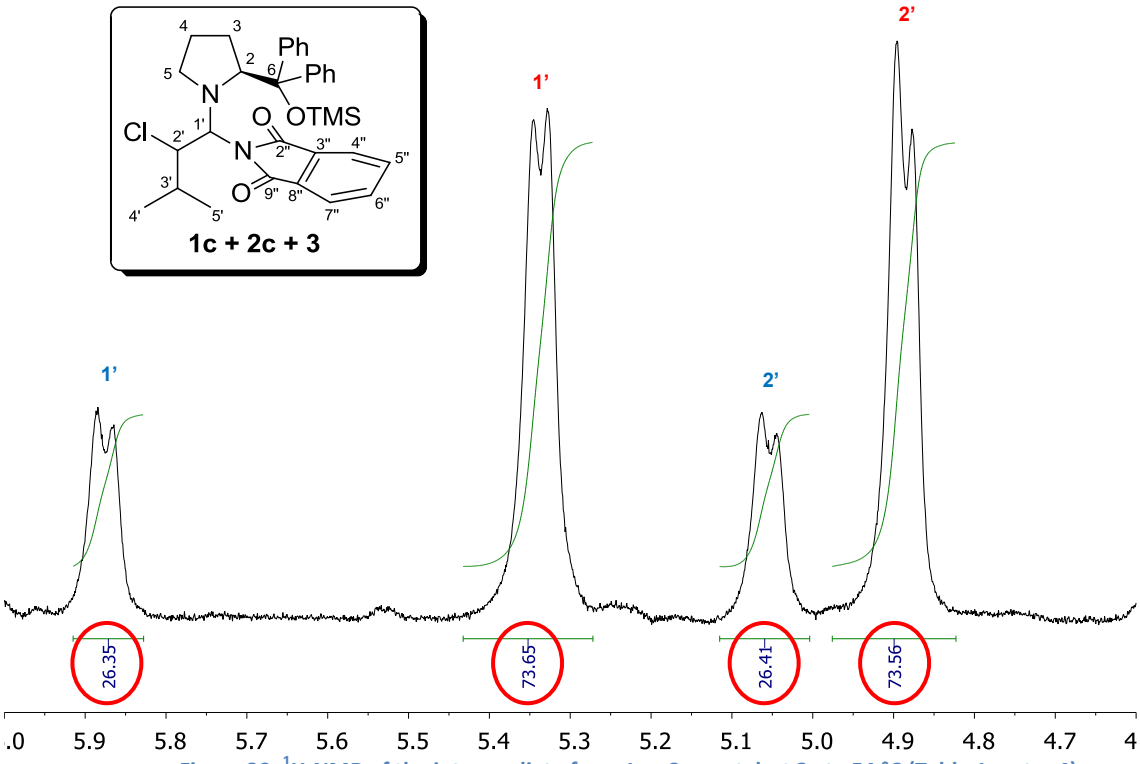

Figure 30. ^{1}H-NMR of the intermediate from 1c + 2c + catalyst 3 at –54 °C (Table 1, entry 4).

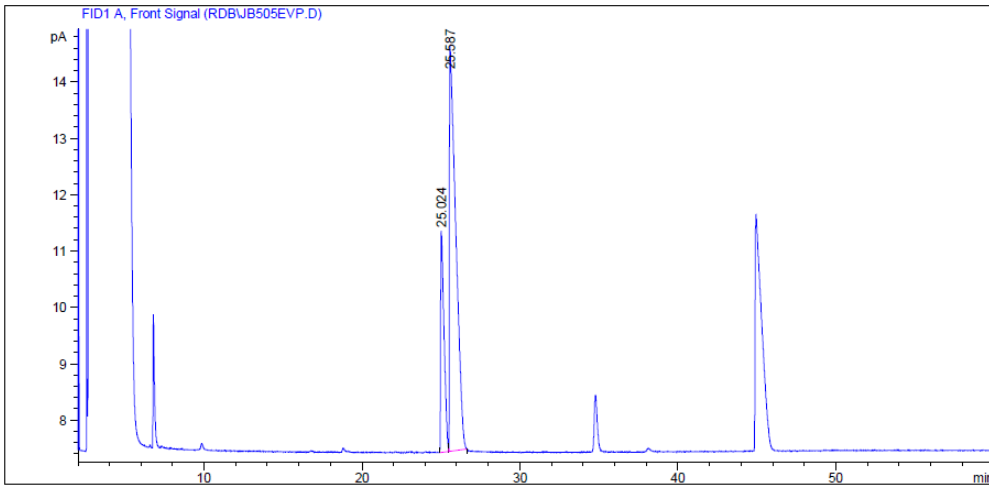


```
=====================================================================
                      Area Percent Report
=====================================================================

Sorted By             :      Signal
Multiplier:                   :      1.0000
Dilution:                     :      1.0000
Use Multiplier & Dilution Factor with ISTDs


Signal 1: FID1 A, Front Signal

Peak RetTime Type  Width     Area      Height     Area
  #   [min]        [min]   [pA*s]      [pA]        %
----|-------|----|-------|----------|----------|--------|
   1  25.024 BV    0.1886   58.79734    3.92848 22.97048
   2  25.587 VB    0.3346  197.17175    7.19826 77.02952
```

Figure 31. Chiral GC of the product of reaction between 1c and 2c, catalyzed by 3 from 0 °C to rt (Table 1, entry 4).

10.6. Intermediate from: 1c + 2c + catalyst 12

In this case only one diastereoisomer was detected even at low temperatures (–54 °C).

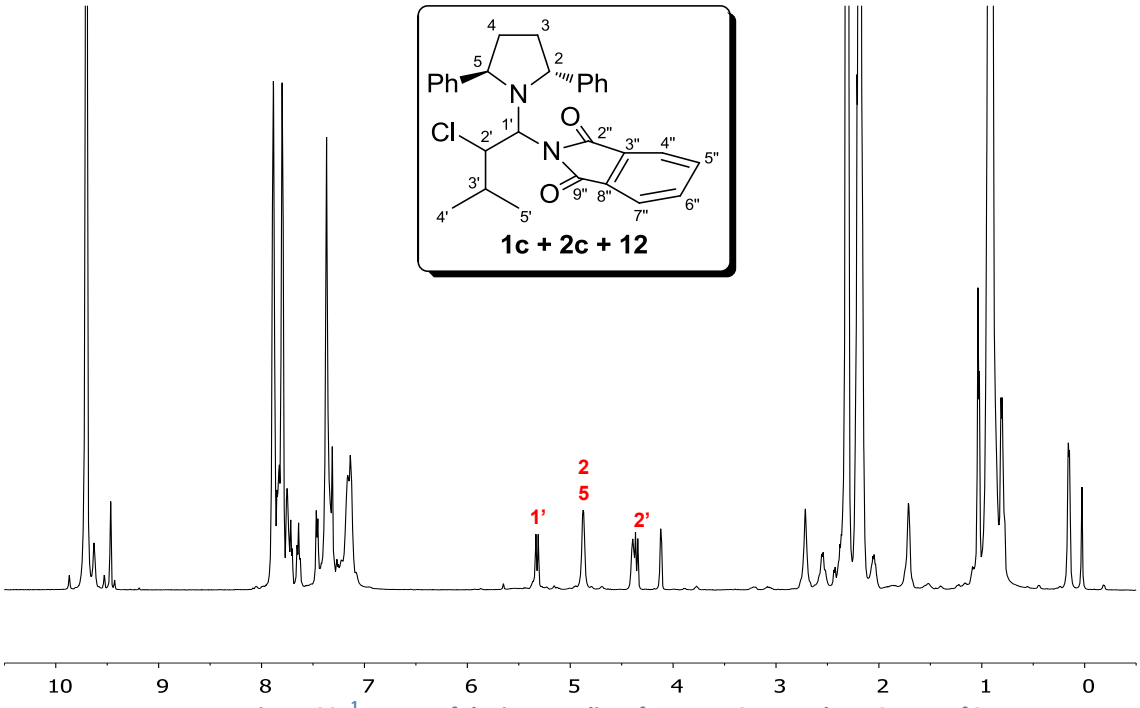

Figure 32. ^{1}H-NMR of the intermediate from 1c + 2c + catalyst 12 at –54 °C.

In addition, there is not any shift of the signals corresponding to the chlorinated intermediate at different temperatures (observed previously for cat **3** and **11** due to the coalescence effect).

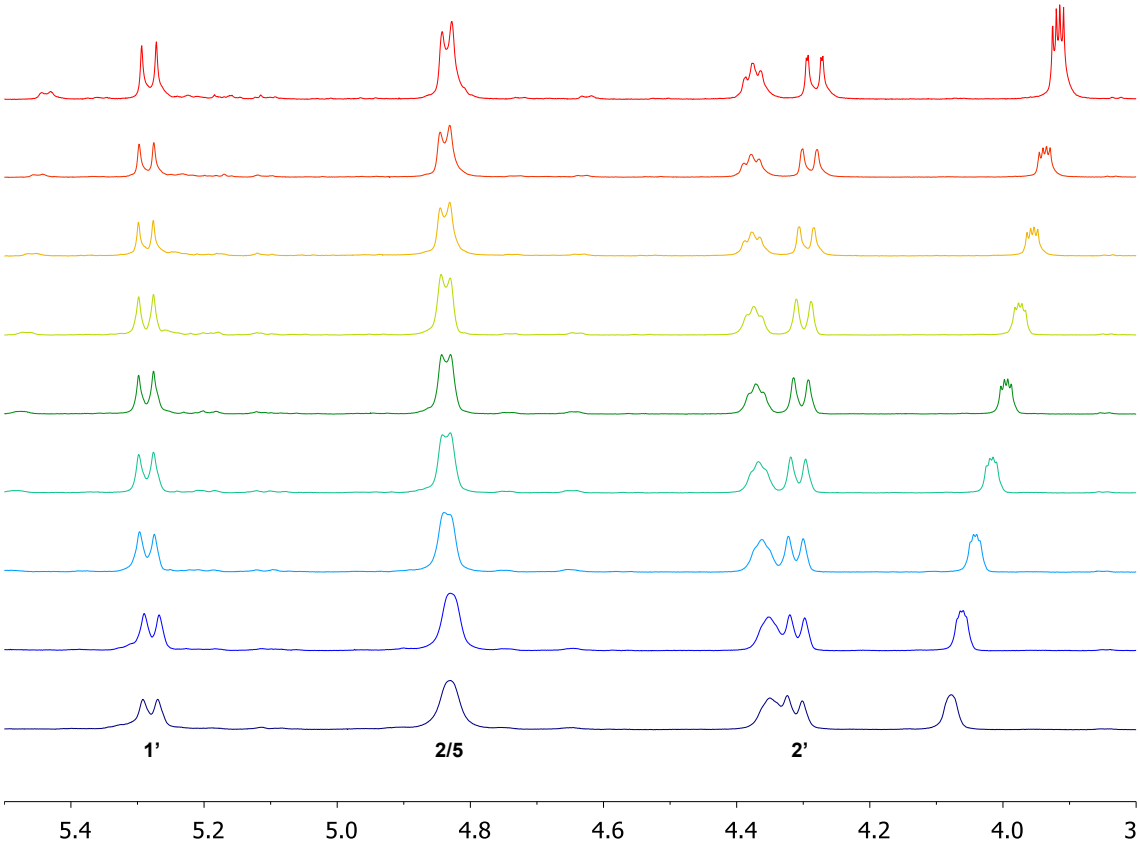

Figure 33. ^{1}H-NMR signals of the intermediate from 1c + 2c + 12 at different temperatures without changes in shifts.

11. NMR of the chlorination reaction

To prove that the intermediates **5c** proceed to the product we performed a reaction with 20 mg of (*S*)-(–)-α,α-Diphenyl-2-pyrrolidinemethanol trimethylsilyl ether (0.06 mmol), 10 mg of isovaleraldehyde (0.12 mmol) and 8 mg of *N*-chlorosuccinimide (0.06 mmol) in 0.6 mL of $CDCl_3$ in the absence of acid.

The spectra in blue shows the formation of the adduct. After the addition of some acid to promote the elimination of the succinimide and the hydrolysis of the corresponding enamine, all the adduct was converted in product (red spectrum).

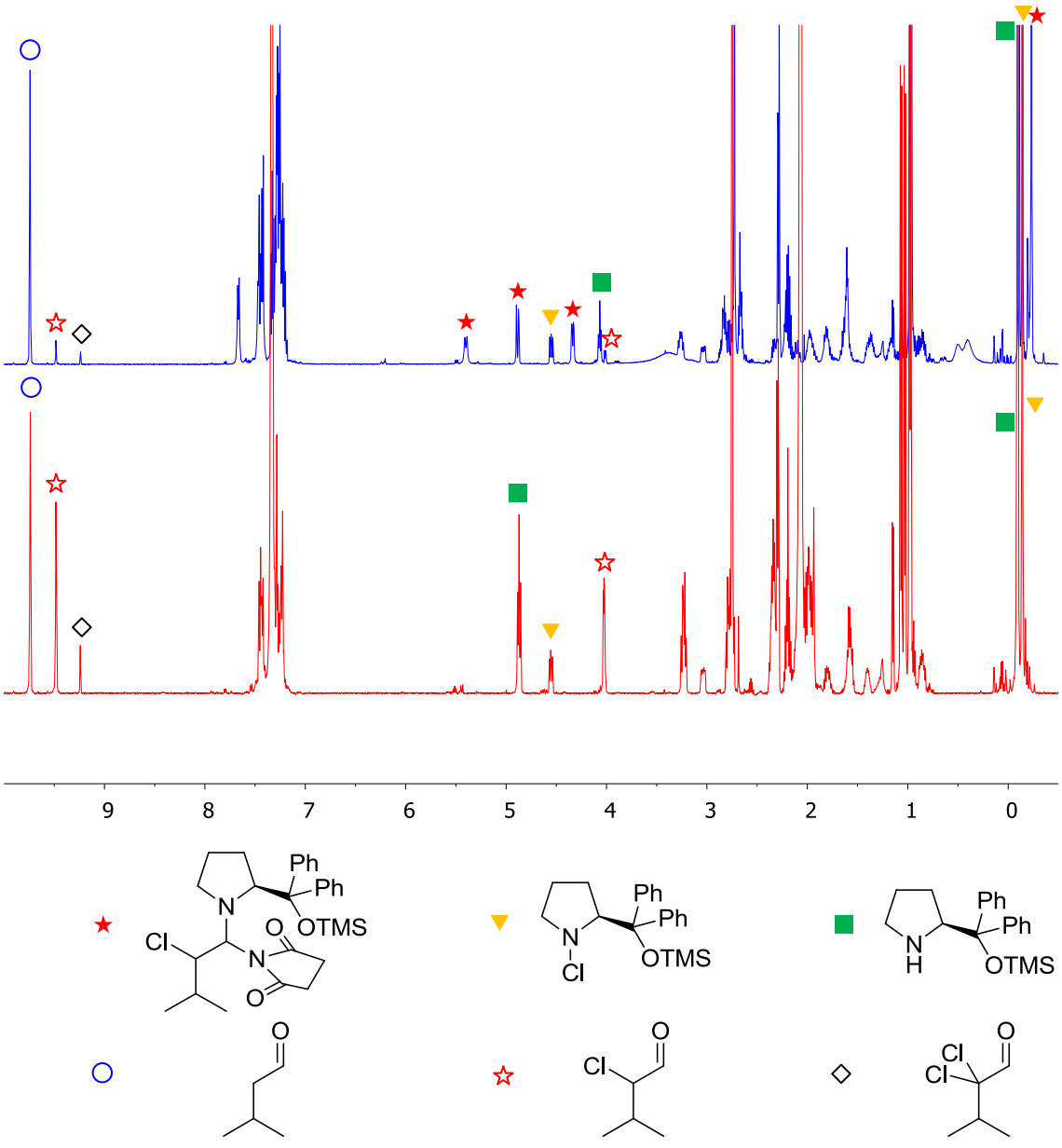

12. Procedure and analysis of α-chlorination reactions

We followed the procedure described in the literature[5] and the spectra were identical to the described.[6] The analysis was done by chiral GC with a column VARIAN CP-ChiraSil-DEX CB 25 x 0.25. Column conditions: He, pressure= 15psi, initial temperature = 30 °C, final temperature = 60 °C, warming rate = 0.5 °C/min, detector temperature = 300 °C, injector temperature = 130 °C. The retention times were aprox.: 30.3 min (*R*) and 30.9 min (*S*).

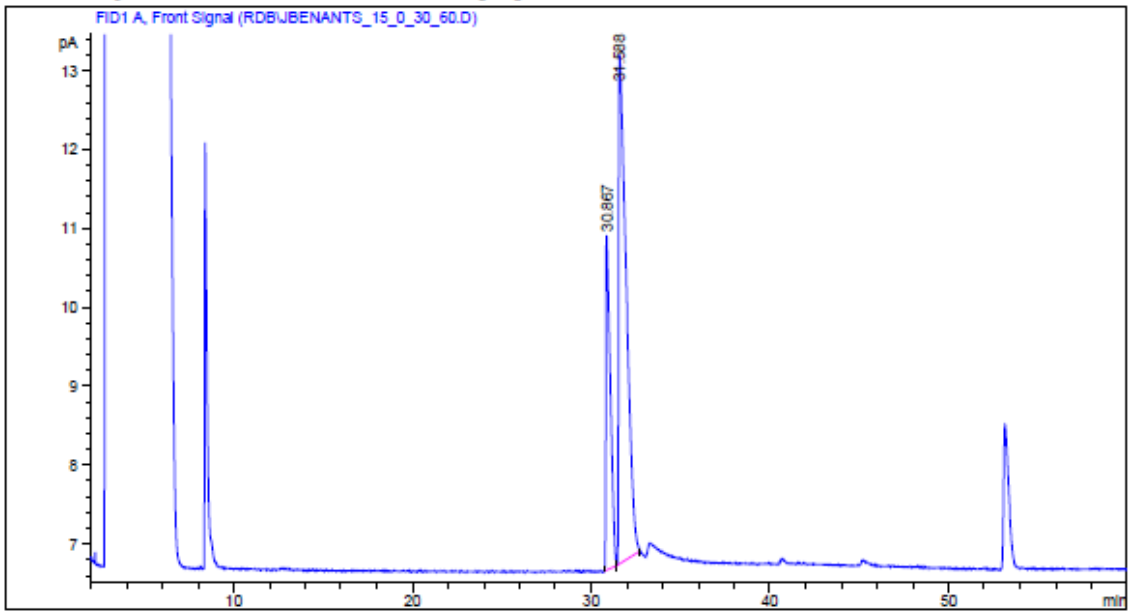


```
================================================================================
                          Area Percent Report
================================================================================

Sorted By             :      Signal
Multiplier:                   :      1.0000
Dilution:                     :      1.0000
Use Multiplier & Dilution Factor with ISTDs


Signal 1: FID1 A, Front Signal

Peak RetTime Type  Width     Area      Height     Area
  #   [min]        [min]   [pA*s]      [pA]        %
----|-------|----|-------|----------|----------|--------|
   1  30.867 BV    0.2283   75.76936    4.24430 28.58682
   2  31.588 VB    0.3462  189.28058    6.45229 71.41318
```

Figure 34. Chiral GC of the product of reaction between 1c and 2b, catalyzed by 3 from 0 °C to rt (Table 1, entry 1).

We also acquired the GC for the product of the reaction catalyzed by **3** at 0 °C. This experiment was done only to check that the *ee* doesn't change if the reaction is run at 0 °C or rt in the same way that we suggest that the ratio between diastereoisomers doesn't change significantly from –54 °C to rt.

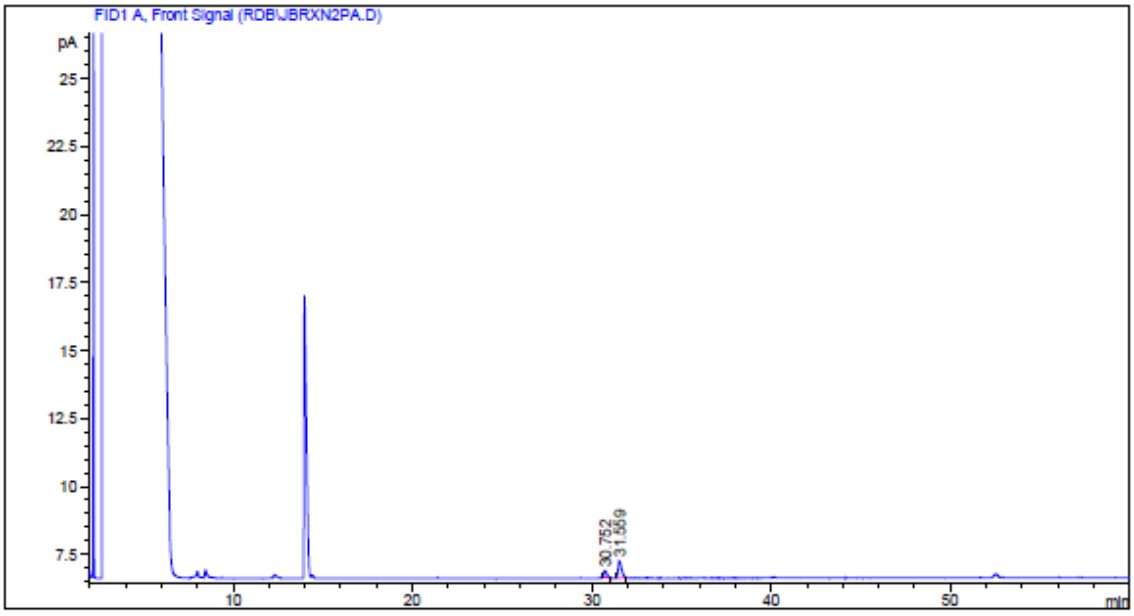


```
=====================================================================
                        Area Percent Report
=====================================================================

Sorted By             :      Signal
Multiplier:                   :      1.0000
Dilution:                     :      1.0000
Use Multiplier & Dilution Factor with ISTDs


Signal 1: FID1 A, Front Signal

Peak RetTime Type  Width     Area      Height     Area
  #   [min]        [min]   [pA*s]      [pA]        %
----|-------|----|-------|----------|----------|--------|
   1  30.752 BV    0.1451    3.24415 2.68160e-1 28.85335
   2  31.559 BB    0.1532    7.99943 6.29590e-1 71.14665
```

Figure 35. Chiral GC of the product of reaction between 1c and 2b, catalyzed by 3 at 0 °C.

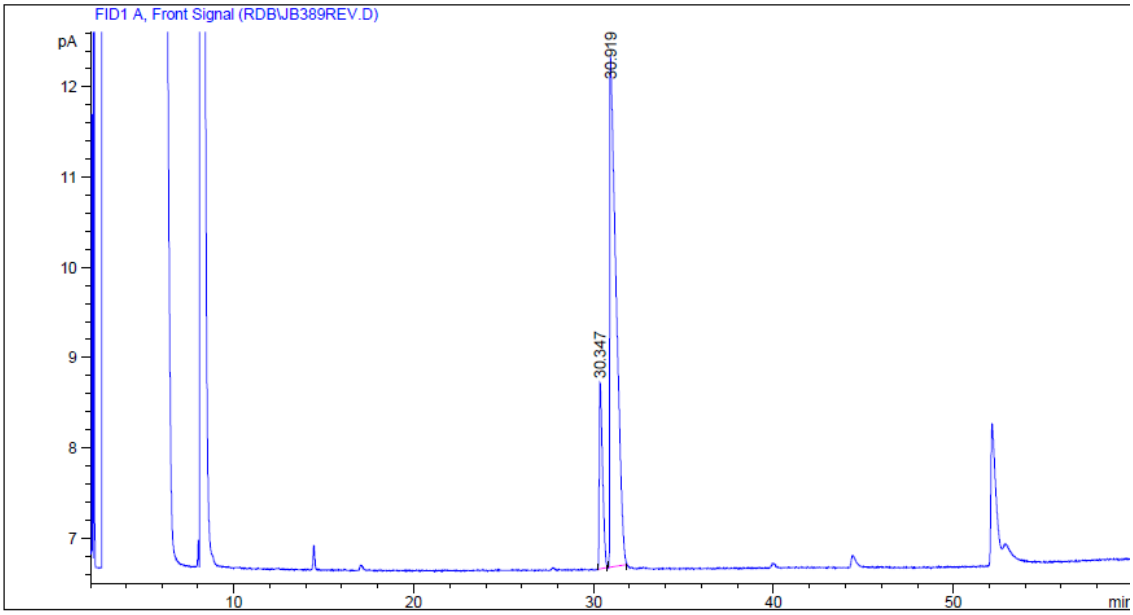


```
================================================================================
                          Area Percent Report
================================================================================

Sorted By             :      Signal
Multiplier:                   :      1.0000
Dilution:                     :      1.0000
Use Multiplier & Dilution Factor with ISTDs


Signal 1: FID1 A, Front Signal

Peak RetTime Type  Width     Area      Height     Area
  #   [min]        [min]   [pA*s]      [pA]        %
----|-------|----|-------|----------|----------|--------|
   1  30.347 BB    0.1630   25.80766    2.06209 15.82733
   2  30.919 BB    0.2944  137.24995    5.68934 84.17267
```

Figure 36. Chiral GC of the product of reaction of 1c and 2b, catalyzed by 11 from 0 °C to rt (Table 1, entry 2).

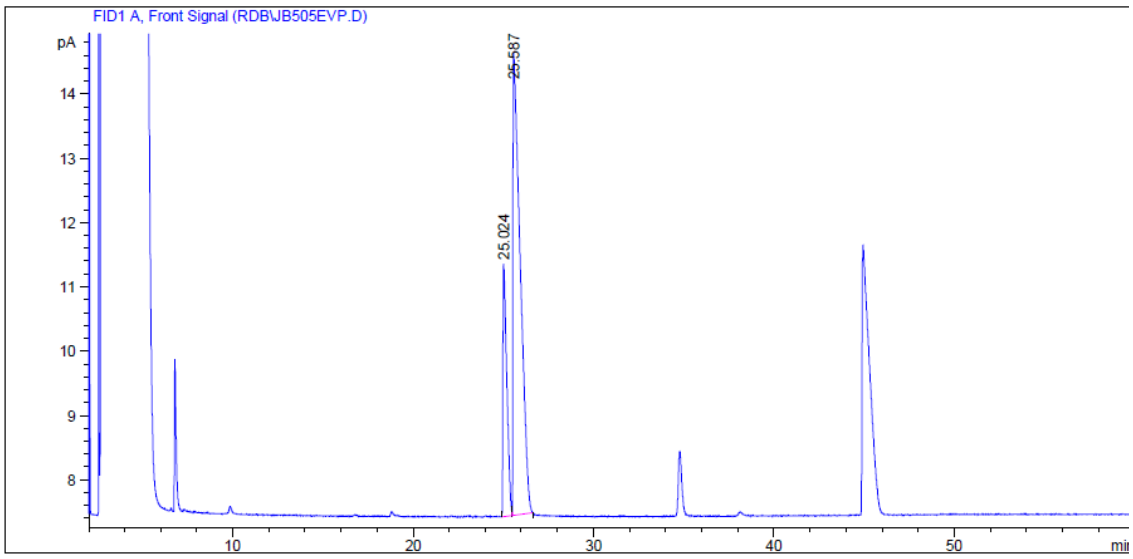


```
=====================================================================
                      Area Percent Report
=====================================================================

Sorted By             :      Signal
Multiplier:                   :      1.0000
Dilution:                     :      1.0000
Use Multiplier & Dilution Factor with ISTDs


Signal 1: FID1 A, Front Signal

Peak RetTime Type  Width     Area      Height     Area
  #   [min]        [min]   [pA*s]      [pA]        %
----|-------|----|-------|----------|----------|--------|
   1  25.024 BV    0.1886   58.79734    3.92848 22.97048
   2  25.587 VB    0.3346  197.17175    7.19826 77.02952
```

Figure 37. Chiral GC of the product of reaction between 1c and 2c, catalyzed by 3 from 0 °C to rt (Table 1, entry 4).

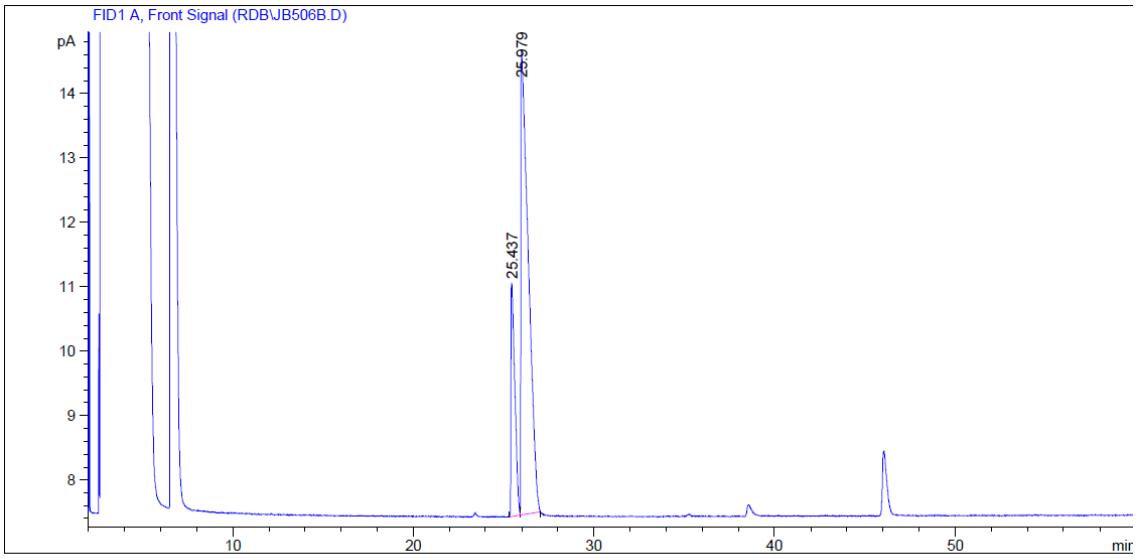


```
=====================================================================
                        Area Percent Report
=====================================================================

Sorted By             :      Signal
Multiplier:                   :      1.0000
Dilution:                     :      1.0000
Use Multiplier & Dilution Factor with ISTDs


Signal 1: FID1 A, Front Signal

Peak RetTime Type  Width     Area      Height     Area
  #   [min]        [min]   [pA*s]      [pA]        %
----|-------|----|-------|----------|----------|--------|
   1  25.437 BV    0.1928   53.83269    3.63385 20.77816
   2  25.979 VB    0.3451  205.25034    7.20977 79.22184
```

Figure 38. Chiral GC of the product of reaction of 1c and 2c, catalyzed by 11 from 0 °C to rt (Table 1, entry 5).

13. Tentative alternative mechanism for α-chlorination reactions

A mechanism may be proposed that is consistent with our experimental data and the published data from Ref. 26b[7] using catalyst **12**.

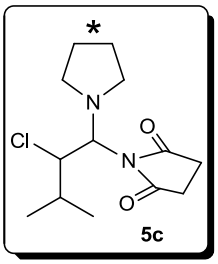

- Two diastereomeric species are in fast equilibrium with the connectivity shown as species **5c** (our work).
- The ratio of concentrations of the diastereomers correlates with the chlorination product enantioselectivity (our work).
- The system obeys overall zero order kinetics (Ref. 26b[7] and our work).
- The nature of the chlorine source has a strong influence on rate, although the reaction is zero order in the concentration of the chlorine source (Ref. 26b[7] and our work).
- The reaction rate is accelerated by acid (Ref 26b[7]).
- The rate is not accelerated by water in the absence of acid (Ref. 26b).

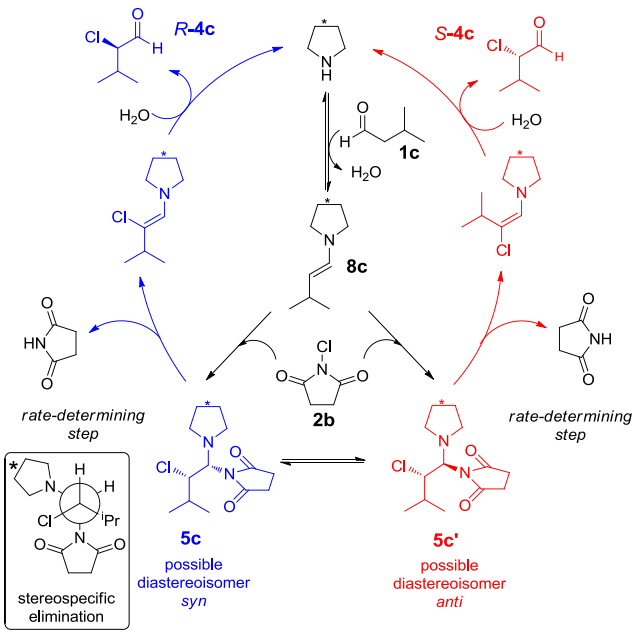

Proposed reaction network. These observations are reconciled by elimination of the succinimide leaving group of **5c** as the rate-determining step (which can be promoted by acid).

Note the kinetic (although not chemical) equivalence of ***intra***- and ***inter***molecular equilibration of the diastereomeric intermediates:

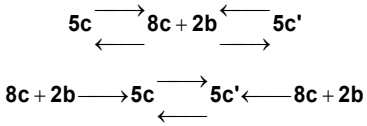

Proposed NMR assignment of diastereomer pairs.

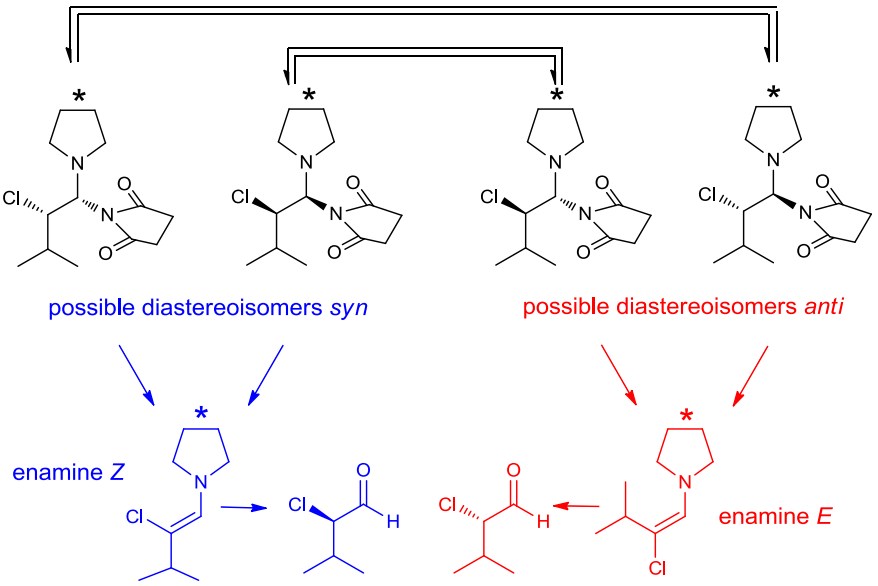

Syn diastereomers lead to *Z*-enamine and *R*-product, *anti* to *E*-enamine and *S*-product. The observed diastereomers correspond to one blue, one red. The stereospecific formation and protonation of enamines of this type has been demonstrated. The assumption of $k_p \approx k_p'$ is in accord with our findings for *E* and Z enamines from a-disubstituted aldehydes and catalysts of type **3**.

Inter vs. intramolecular equilibration of diastereomers. The overall network for equilibration written as fully reversible (microscopic reversibility):

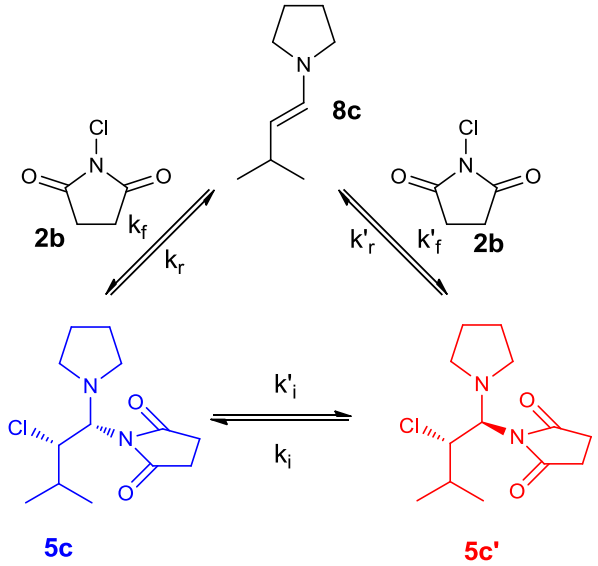

The equilibrium relationships are as follows:

$$k_r[\mathbf{5c}]_{eq} = k_f[\mathbf{8c}]_{eq}[\mathbf{2b}]_{eq}$$
$$k_r'[\mathbf{5c'}]_{eq} = k_f'[\mathbf{8c}]_{eq}[\mathbf{2b}]_{eq}$$
$$k_i'[\mathbf{5c}]_{eq} = k_i[\mathbf{5c'}]_{eq}$$

This gives the following relationships between the rate constants:

$$k_f \cdot k_r' \cdot k_i' = k_f' \cdot k_r \cdot k_i$$
$$\frac{[\mathbf{5c}]_{eq}}{[\mathbf{5c'}]_{eq}} = \frac{k_i}{k_i'} = \frac{k_f}{k_f'} \cdot \frac{k_r'}{k_r}$$

Thus the equilibration between the diastereomers may be described by either the intermolecular route or the intramolecular route. If the addition of **2b** is driven strongly forward (k_r, k'_r both very small), but the direct intramolecular interconversion is facile, the kinetic consequence is identical to having a fast reversible addition of **2b** to **8c** and slow intramolecular interconversion.

14. Characterization of the intermediate in the Michael reaction with maleimide

20 mg (0.06 mmol) of (*S*)-α,α-diphenyl-2-pyrrolidinemethanol trimethylsilyl were added to a solution of 42 mg (0.72 mmol) of propanal and 104 mg (0.60 mmol) of *N*-phenylmaleimide in 0.6 mL of $CDCl_3$ in a NMR tube at room temperature. Immediately, NMR spectra were registered in a 600 MHz spectrometer.

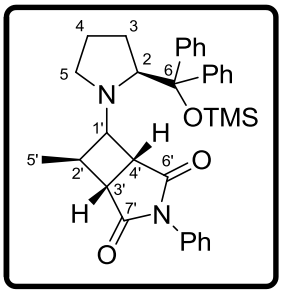

(1*R*,5*R*,7*R*)-6-((*S*)-2-(diphenyl((trimethylsilyl)oxy)methyl)-pyrrolidin-1-yl)-7-methyl-3-phenyl-3-azabicyclo[3.2.0]heptane-2,4-dione: **^{1}H-NMR** (600 MHz, $CDCl_3$) δ –0.18 (s, 9H; OTMS), 0.65–0.78 (m, 1 H; C(4)H), 0.97–1.05 (br, 3H; C(5')H), 1.37–1.47 (m, 1 H; C(4)H), 1.76–1.90 (m, 1 H; C(3)H), 1.95–2.07 (m, 1 H; C(3)H), 2.64–2.75 (m, 2 H; C(5)H), 2.80–2.90 (m, 1 H; C(2')H), 3.16 (dd, 1 H, *J* = 10.8, *J* = 7.0; C(3')H), 3.53 (dd, 1 H, *J* = 7.0, *J* = 5.2; C(4')H), 4.13 (dd, 1 H, *J* = 9.5, *J* = 2.9; C(2)H); **^{13}C-NMR** (150.9 MHz, $CDCl_3$) δ 178.6 (C6'/C7'), 176.3 (C6'/C7'), 84.0 (C6), 69.5 (C1'), 68.3 (C2), 47.9 (C5), 40.2 (C4'), 37.6 (C3'), 36.1 (C2'), 28.7 (C3), 23.3 (C4), 15.8 (C5'), 1.8 (OTMS).

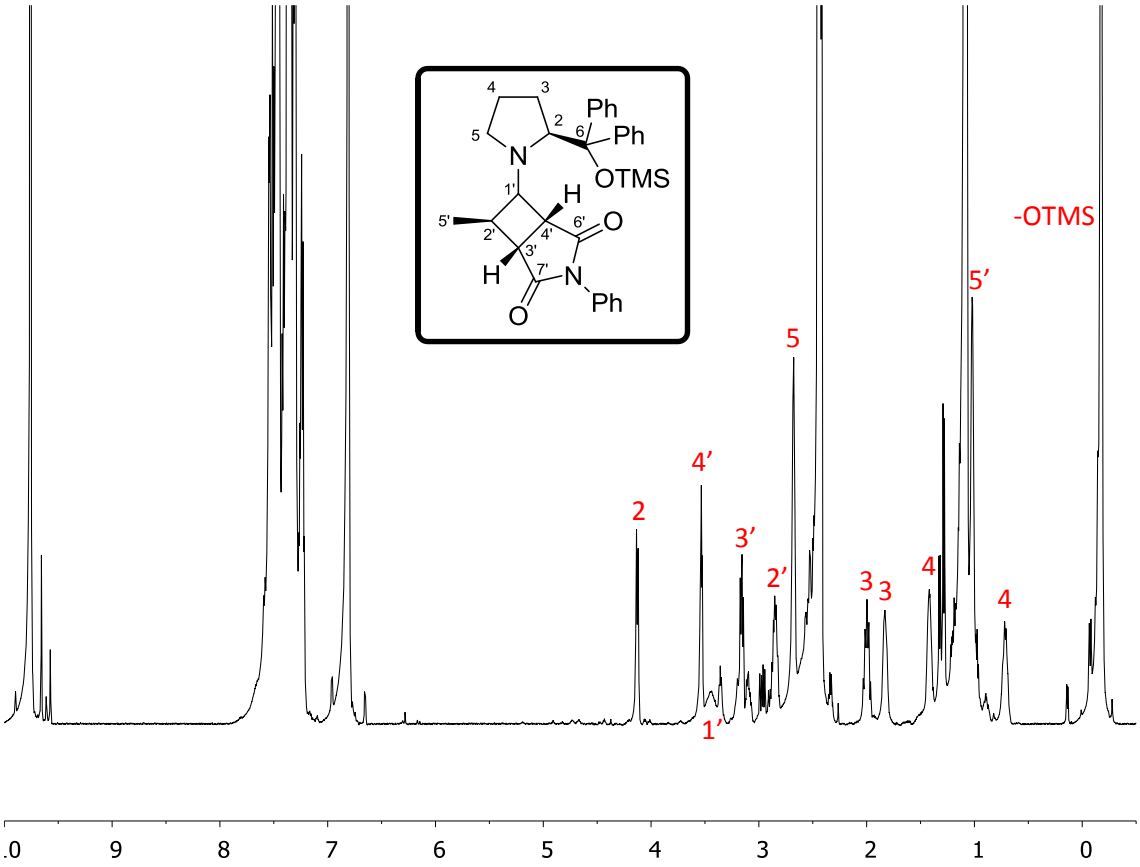

Figure 39. ^{1}H-NMR of the intermediate in the Michael reaction with maleimide.

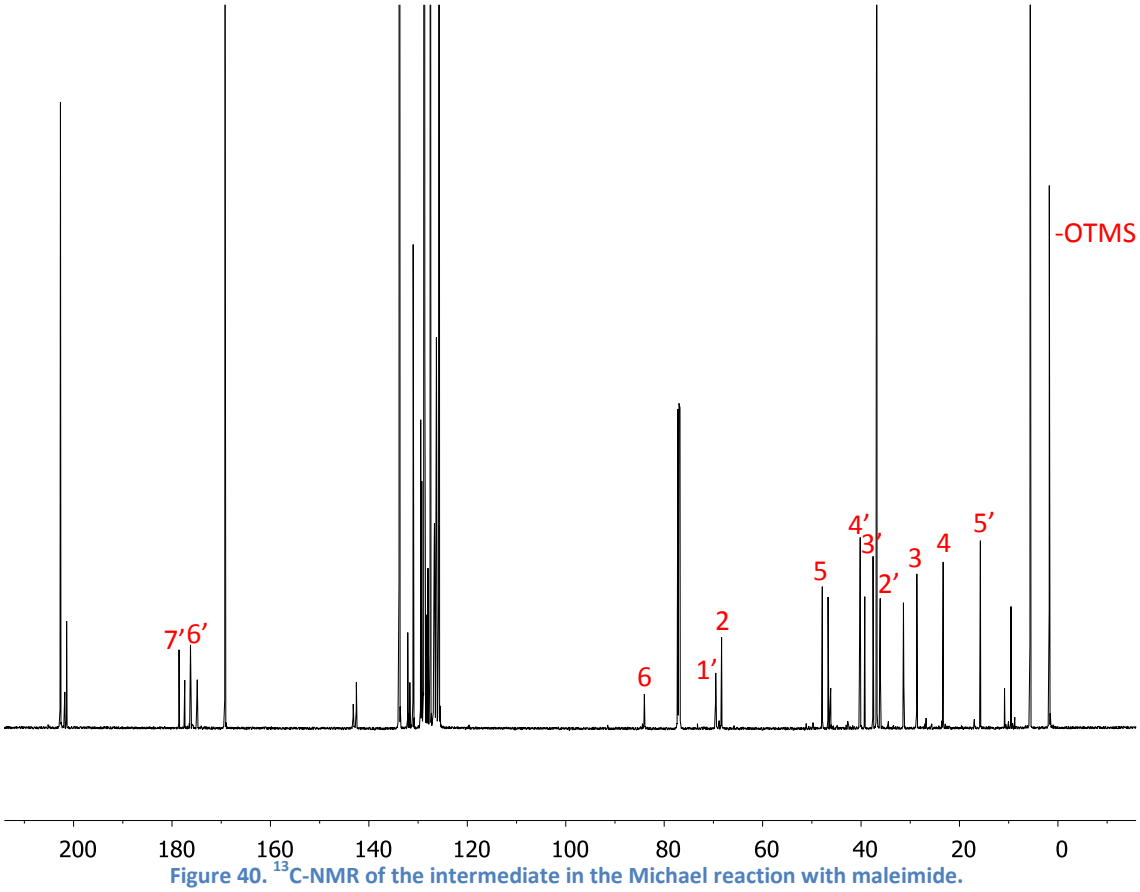

Figure 40. ^{13}C-NMR of the intermediate in the Michael reaction with maleimide.

The assignment of the molecule is based on the two dimensional experiments shown below.

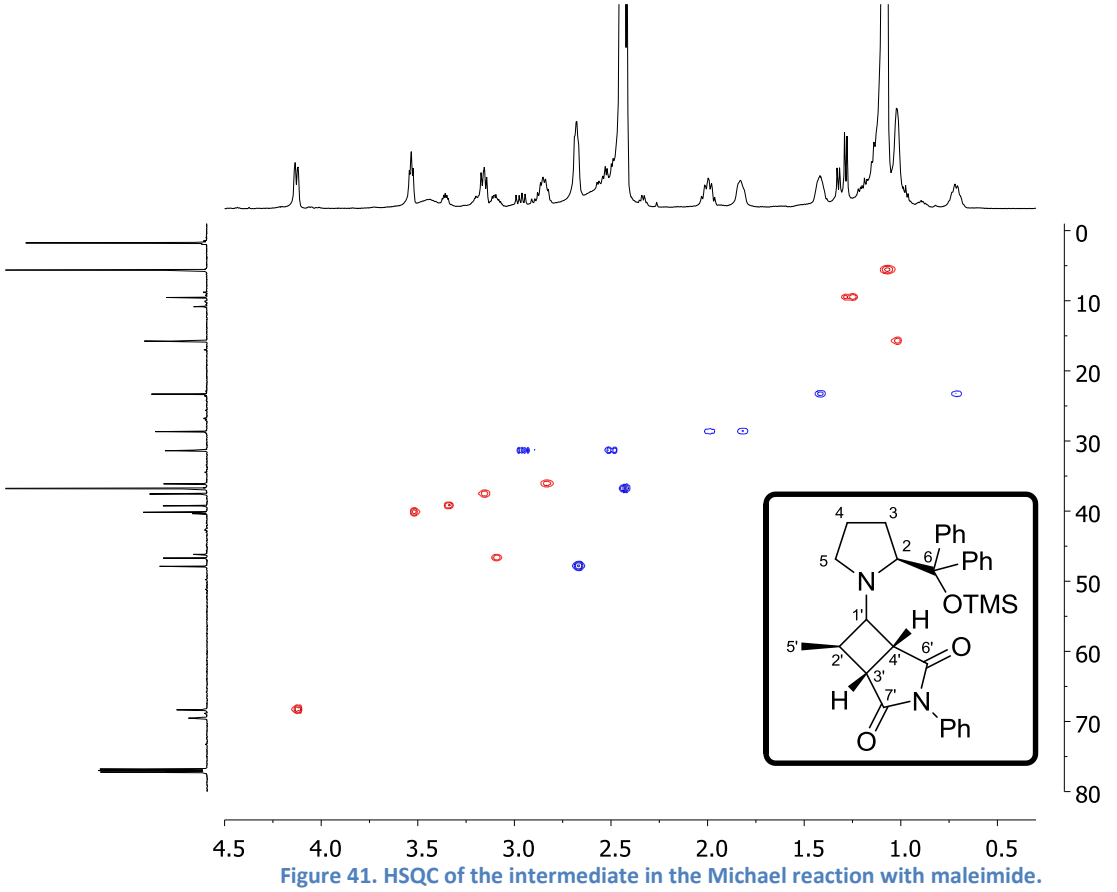

Figure 41. HSQC of the intermediate in the Michael reaction with maleimide.

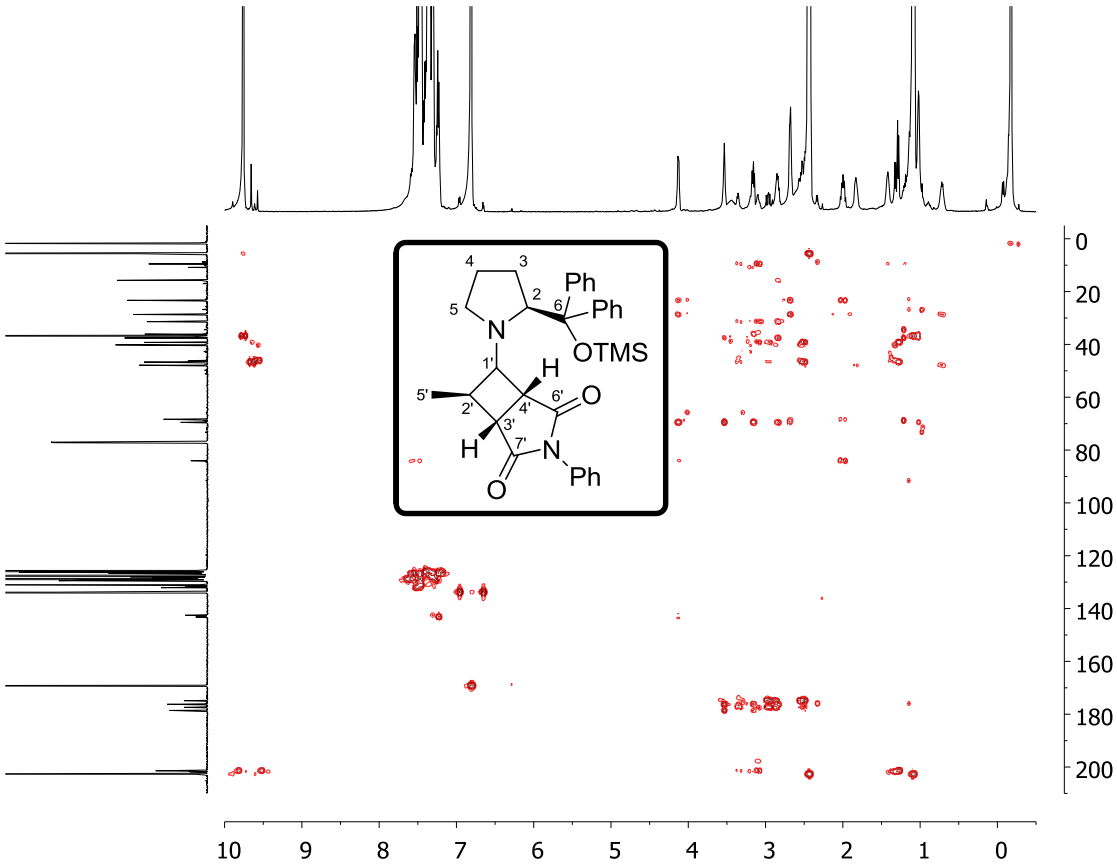

Figure 42. HMBC of the intermediate in the Michael reaction with maleimide.

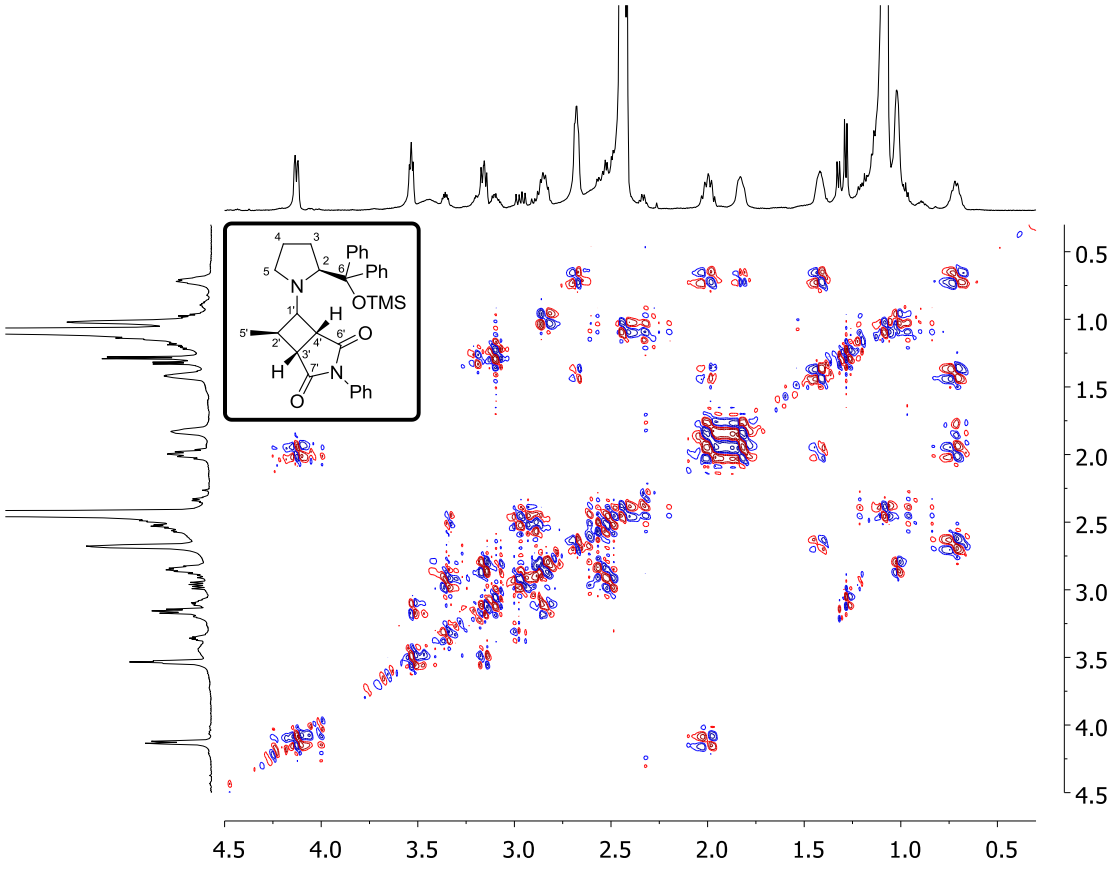

Figure 43. COSY of the intermediate in the Michael reaction with maleimide.

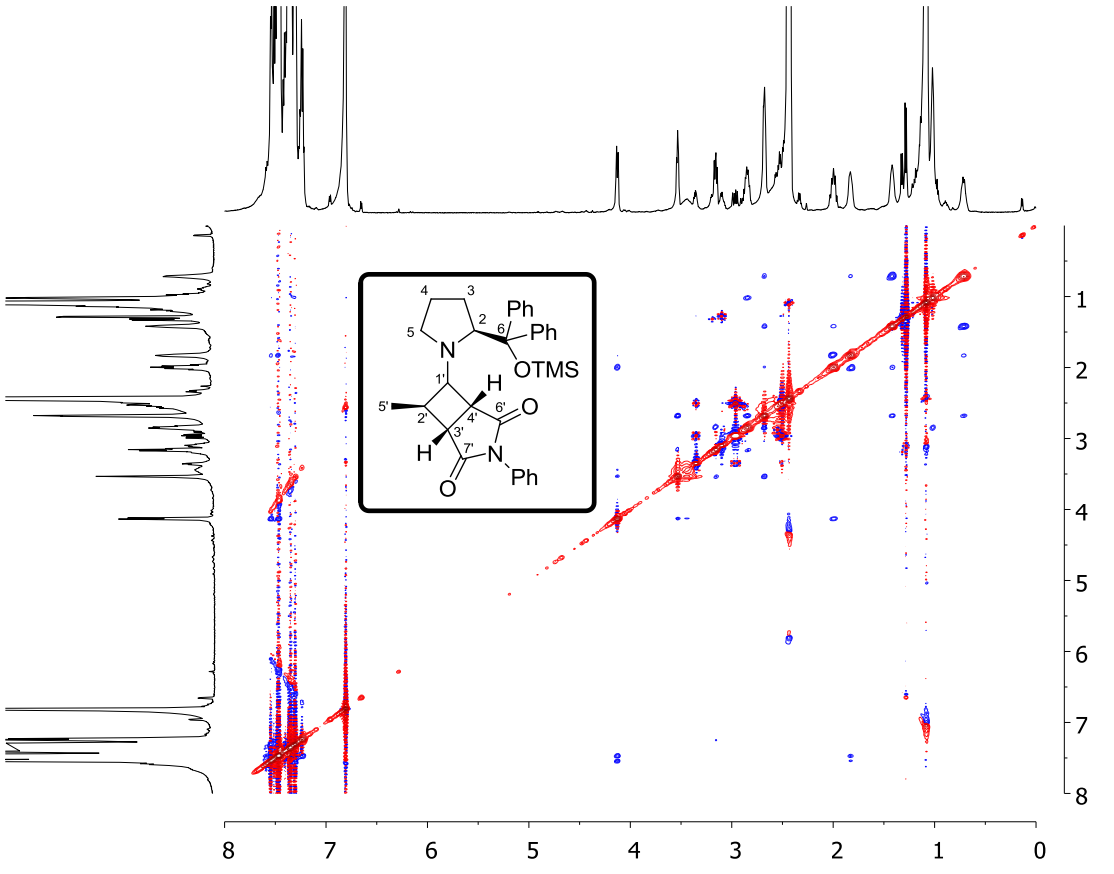

Figure 44. NOESY of the intermediate in the Michael reaction with maleimide.

15. Bibliography

1. D'Aniello, M. J.; Barefield, E. K., Mechanistic studies on the catalysis of isomerization of olefins by (Ph3P)3NiX. *J. Am. Chem. Soc.* **1978,** *100* (5), 1474-1481.
2. Burés, J.; Armstrong, A.; Blackmond, D. G., Mechanistic Rationalization of Organocatalyzed Conjugate Addition of Linear Aldehydes to Nitro-olefins. *J. Am. Chem. Soc.* **2011,** *133* (23), 8822-8825.
3. Hoops, S.; Sahle, S.; Gauges, R.; Lee, C.; Pahle, J.; Simus, N.; Singhal, M.; Xu, L.; Mendes, P.; Kummer, U., COPASI—a COmplex PAthway SImulator. *Bioinformatics* **2006,** *22* (24), 3067-3074.
4. IUPAC. Compendium of Chemical Terminology, 2nd ed. (the "Gold Book"). Compiled by A. D. McNaught and A. Wilkinson. Blackwell Scientific Publications, Oxford (**1997**). XML on-line corrected version: http://goldbook.iupac.org (**2006**) created by M. Nic, J. Jirat, B. Kosata; updates compiled by A. Jenkins. ISBN 0-9678550-9-8. doi:10.1351/goldbook.
5. Halland, N.; Braunton, A.; Bachmann, S.; Marigo, M.; Jorgensen, K. A., Direct Organocatalytic Asymmetric α-Chlorination of Aldehydes. *J. Am. Chem. Soc.* **2004,** *126* (15), 4790-4791.
6. Craig, D.; Harvey, J. W.; O'Brien, A. G.; White, A. J. P., Exopericyclic stereocontrol in Johnson-Claisen rearrangements of allylic sulfides. *Chem. Commun. (Cambridge, U. K.)* **2010,** *46* (37), 6932-6934.
7. Halland, N.; Alstrup Lie, M.; Kjærsgaard, A.; Marigo, M.; Schiøtt, B.; Jørgensen, K. A., Mechanistic Investigation of the 2,5-Diphenylpyrrolidine-Catalyzed Enantioselective α-Chlorination of Aldehydes. *Chemistry – A European Journal* **2005,** *11* (23), 7083-7090.